Bauhaus-Universität Weimar
Faculty of Media
Degree Programme Human Computer Interaction

Shaketrack

Comparing sensor locations for acceleration based handshake matching

Master's Thesis

Andreas Berst
born on 12.05.1990 in Würzburg

Matriculation number: 114789

First referee: Junior-Prof. Dr. Florian Echtler
Second referee: Prof. Dr. Ing. Eva Hornecker

Submission date: 03.11.2017

Declaration of Authorship

I hereby declare that I have written this thesis without the use of documents and aids other than those stated in the references, that I have mentioned all sources used and that I have cited them correctly according to established academic citation rules, and that the topic or parts of it are not already the object of any work or examination of another study program.

Date | Andreas Berst

Abstract

The digitalization of physical gestures is a growing field of research. Especially, greeting gestures pose the opportunity for interesting applications. One commonly known example is the exchange of contact information by just performing a handshake gesture.

Other researchers have examined multiple ways to improve this procedure and propose various methods. Some of these approaches utilize the motion of the hand to ensure a directed data transfer. However, during previous research, it was observed that the way people tense their wrist during a handshake can have a great impact on the performance of these systems. The goal of this thesis is to explore a different sensor location to find a system that is less dependent on the wrist tension.

Therefore, this thesis investigates and compares the resemblance of acceleration signals for wrist and finger mounted sensors in the handshake scenario. During the course of this examination, a custom hardware setup was developed. It was used to gather a dataset of 90 unique handshakes for further analysis. The results indicate that the sensor located on the wrist generated signals with greater similarity.

Contents

1 Introduction

This chapter leads the reader to the research question addressed in this thesis. Section 1.1 introduces the handshake as a greeting gesture and explains its role, usage and context. To explain the motivation behind handshake related research, Section 1.2 discusses how the properties of this gesture can be utilized for an application. Finally, Section 1.3 highlights the goals and explains the structure of this thesis.

1.1 Shaking hands - a simple greeting gesture

When humans meet face to face, greeting gestures are an essential part of their interaction. Obviously, there are many non-verbal expressions that frame such an encounter. They can take different forms depending on the culture, social relationship, gender and other factors [1][2]. In the western world, one of the most common gestures during a face to face meeting is the handshake. The following reference should serve as a definition for this particular gesture and create a common ground for further considerations:

> ”Handshake — a grasping with the right hand of another’s right hand or a grasping of right hands by two people often with a slight up and down shake of the hands usually upon meeting or taking leave as a sign of friendship, affection, or good wishes or as a mere polite formalty.” [3]

Within this definition, the handshakes can vary in duration, intensity of the movement, force of the grip and in the frequency of the up and down movement. These differences are also influenced by the cultural background, a person’s gender, the setting and the occasion of the encounter [4]. Considering that the grip creates a physical coupling, both parties generate a unique movement based on these circumstances.

1.2 Handshakes in the digital age

In a time where technology with all its advantages and disadvantages is intertwining with almost every part of our lives, commonly used gestures like the handshake become particularly attractive for the deployment of technology. In fact, since the introduction of the smartphone, mobile computing has become an important field of research and development. With the increasing availability of smartwatches, smartbands, and other wearables, there is a growing market for applications that make use of these new devices.

In the context of digitalization, the handshake offers some particularly interesting properties. Since it is used as a greeting gesture, it represents an initial or conclusive mark during a face to face meeting. Moreover, the gesture contains a distinct shared motion sequence that can be measured and digitally processed. In addition, it implies physical contact and requires the two interacting persons to stand closely together. Hence, the handshake provides the opportunity to utilize technologies for low proximity or contact-based data transfer. All these properties can be salvaged to develop interaction-based applications.

It is a very prominent idea, to use the handshake as a trigger to launch the exchange of data between mobile devices. This usage scenario is currently patent-protected by Apple Inc. [5] and has been the motivation for several research projects.

For example, Hickenly [6] investigated the concept of using gestures to trigger the exchange of information. He used a synchronous bumping gesture between two displays to connect both devices and share information between them. Another gesture related system was presented with the IBand [7]. This wrist-mounted device was built to exchange information between two people who perform a handshake gesture. After the devices detected an up-and-down movement of the equipped hands, the IBands initiated an infrared data transfer.

When employing the handshake for the exchange of data, one has to face two main challenges. At first, the gesture has to be tracked and recognized by the system to trigger the data exchange. After a successful detection, the system has to provide a way of exchanging data between the involved parties. Some systems, like the IBand, use a directed transfer technology to ensure a targeted data exchange between interacting persons.

As the handshake includes physical contact, touch-based transfer technologies offer an additional way of data exchange. A good example was given by Zimmerman [8]. He used the conducting property of the human body to transfer data between the interacting users.

In contrast to the directed approach, broadcast or network based transfer technologies like Bluetooth and WiFi need an additional differentiator. This supplementary mechanism is crucial to ensure only corresponding parties are taking part in the data exchange. It is a common approach to salvage the synchronized movement of the gesture to match corresponding handshakes. For instance, Auguimeri et. al [9] presented a system for interaction based data transfer using body sensor networks. They utilized decision trees to classify and match acceleration signals that were generated by two persons performing a common handshake. Still, this system required a pre-existing connection to transfer the signal data to the partner device.

In contrast, the Shakecast [10] application proposed a solution that uses several features computed from the acceleration data of a handshake to directly encode a Bluetooth Low Energy (BLE) data broadcast. Hence, the system did not need to transfer any signal data to the partner device. Therefore, it works as a peer-to-peer(P2P) solution and does not need a pre-existing network connection.

1.3 Goal of this thesis

Most of the earlier described acceleration based solutions require a lot of computational effort. The sensor data is constantly copied, transformed and compared. Therefore other disambiguation mechanisms seem preferable. Based on this assumption Chapter 2 describes a simple experiment that was carried out during the exploratory phase of this thesis. The experiment was conducted to explore Near-Field-Communication(NFC) as a tool to ensure directed handshake based data exchange.

This thesis can be seen as a followup on the Shakecast application. Therefore, the main inquisition is based on an observation that was made during the project. It was observed, that the way testers strained their wrist had a great impact on the acceleration signal. In some cases, this difference in joint tension even led to unmatchable handshake data. It is assumed that this joint induced disparity also affected the overall performance of the application.

This thesis investigates this circumstance while searching for a possible solution for the disparity problem. By moving the sensors to the finger of a user and therefore beyond his wrist the observed joint-induced disparity should be reduced. Accordingly, this thesis examines if the corresponding acceleration signals of a finger based system have a higher resemblance than the signals of a wrist based system.

In order to substantiate the impact of this alternate sensor position Chapter 3 suggests several features that can be computed from acceleration data. Furthermore, several similarity measures are introduced and some challenges of signal matching are discussed. Chapter 4 presents a custom hardware setup that was developed to create a dataset for the comparison of two different sensor positions. In Chapter 5, the data acquisition process is explained. Additionally, this chapter provides some additional information about the metrics of the dataset.

Thereafter, Chapter 6 introduces the analysis tool that was developed to compute the similarity measures. Moreover, it contains the results of the signal similarity analysis for both sensor locations as well as the concluding comparison. Finally, Chapter 7 discusses the results of the preceding analysis and highlights important findings. Additionally, some insights and ideas for future research are presented.

2 Exploration of Near Field Communication (NFC)

This chapter presents some insights from the exploratory phase of this thesis. Section 2.1 starts with a short overview of the Near Field Communication (NFC) technology. Afterwards, Section 2.2 describes an experiment that was conducted to investigate the applicability of this technology to the developments of the intended handshake system. Consequently, Section 2.3 summarizes and evaluates the obtained results of this experiment.

2.1 NFC, a proximity-based transfer technology

Within the last years, NFC became popular as a technology for mobile payment and is commonly used for digital key cards. The protocol belongs to a subset of the RFID standard. Therefore, it uses inductive coupling to transfer data between two respective devices. NFC, in particular, operates in the high frequency band at 13.56 MHz and supports wireless data transfers with a rate of 424 kbits per second in a range up to 10 cm [11].

Since the handshake gesture provides a mutual close range space between two persons, NFC seems to be a viable technology to explore in this context. Considering a transmission range of 10 cm, one can find several mounting points for NFC devices to interact during a handshake. To explore the possible application of NFC in the context of this gesture, a simple experiment was conducted. The goal was to determine a suitable mounting location on the hand that would enable a stable data transfer between two NFC devices.

2.2 Experiment: NFC readings in different scenarios

This experiment was realized with a PN532 NFC RFID modules [12] and the passive NFC Tag of the NRF52. Both were put in a certain position in relation to the hands of the participants. After the positioning, the circumstances of a handshake were simulated, while the output of the active device was monitored for successful readings. This procedure was repeated three times. Each time, the position of the NFC devices was changed to an alternate position.

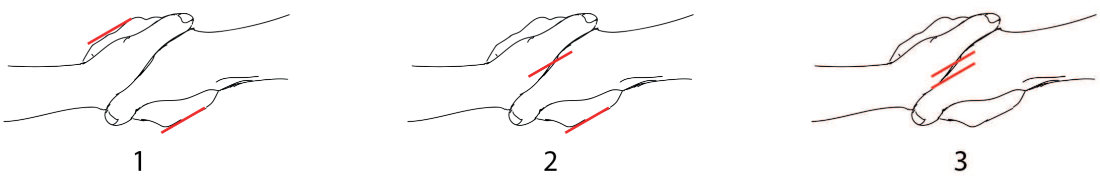

Figure 2.1: Exemplary sketch of the NFC device locations during the exploration. The red line represents the approximate positioning of the devices.

As shown in Figure 2.1, the modules were first positioned at the back sides of the participants' right hands. For the second iteration, for one of the devices was positioned between the hands of the participants. Therefore, the distance between the two NFC devices was reduced. During the third trial, both NFC devices were placed on the palms of the participants.

2.3 Evaluation of NFC for handshake based data exchange

During the first two trials, the active module was not able to register any data exchange. However, in the third scenario, the reading of the data was successful. As a result, it seems plausible that in the first two cases, the human hand acted as an electromagnetic shield between the two devices and obstructed the exchange. Only during the last scenario of the experiment, the inductive coupling was strong enough due to the low distance and no shielding obstacle.

This bears the implication that at least the antenna of a NFC device would need to be worn on the inside of the hand if this technology is utilized to trigger gesture-based data exchange or even as a transfer technology for application data. Still, it is questionable whether this is a usable approach in a real-world scenario due to the physical size of an antenna. Such a device would be a disturbance when performing a handshake if not fitted in an unobtrusive way. It might be an idea worth pursuing, to fit the hardware into the form of a common ring. However, it is undetermined if NFC devices that are wrapped around the fingers would provide enough inductive linkage in a handshake scenario.

Due to its susceptibility to the electromagnetic shielding of the human body, NFC does not seem to be a suitable approach to enable handshake based data exchange. However, when combined with other approaches, RFID or NFC in specific could help to ensure that corresponding handshakes are matched by enforcing close proximity. Therefore, it is still valid to explore its application in future research.

3 Digitalization of a handshake

After concluding the NFC exploration, the focus of this thesis shifted to the investigation of an alternative sensor position to acquire acceleration signals of greater resemblance. Therefore, Section 3.1 begins with a short discussion of different sensor positions. Afterwards, Section 3.2 provides a short introduction into the possible measurements of an inertial sensor and shows several features that can be derived from an acceleration signal. Section 3.3 describes a number of problems that can arise during the comparison of acceleration data. Afterwards, Section 3.4 explains the similarity criteria, which can be used for the evaluation. Finally, Section 3.5 demonstrates how the different similarity measures are altered by preprocessing steps like smoothing and signal segmentation.

3.1 Selection of a sensor position

A handshake can be segmented in four phases [13]. First, there is an initial movement to bring the hands together. It is followed by a short period of unsynchronized movement to counterbalance the initial movement and the physical contact. In the next phase, the two interacting persons engage in a synchronized motion. Finally, the gesture is completed by releasing the hands.

To utilize these phases, especially the one containing the synchronized movement many approaches employ inertial sensors at the wrists of the interacting persons [10][14]. This location has two convenient properties. First of all, a wrist mounted sensor is not within the area of physical contact. Therefore, it does not obstruct the gesture in any way. Second, it is very common to wear watches or trinkets on the wrist. Especially when thinking about user-centered consumer applications this is a beneficial quality.

However, as stated during the introduction, measurement data acquired at this position is influenced by the way people tense up their wrist joint. By attaching the sensor to the finger, instead of the wrist this effect could be reduced. Based on this assumption, the acceleration data of an inertial sensor worn like an ordinary ring is investigated.

3.2 Measurements

A deployed IMU provides the acceleration value for three axes x, y, and z. These values are recorded with a certain sample rate. Depending on the internal settings and the built-in capabilities of a sensor, it can record multiple samples within a second. Consequently, the sensor output can be interpreted as a time series signal.

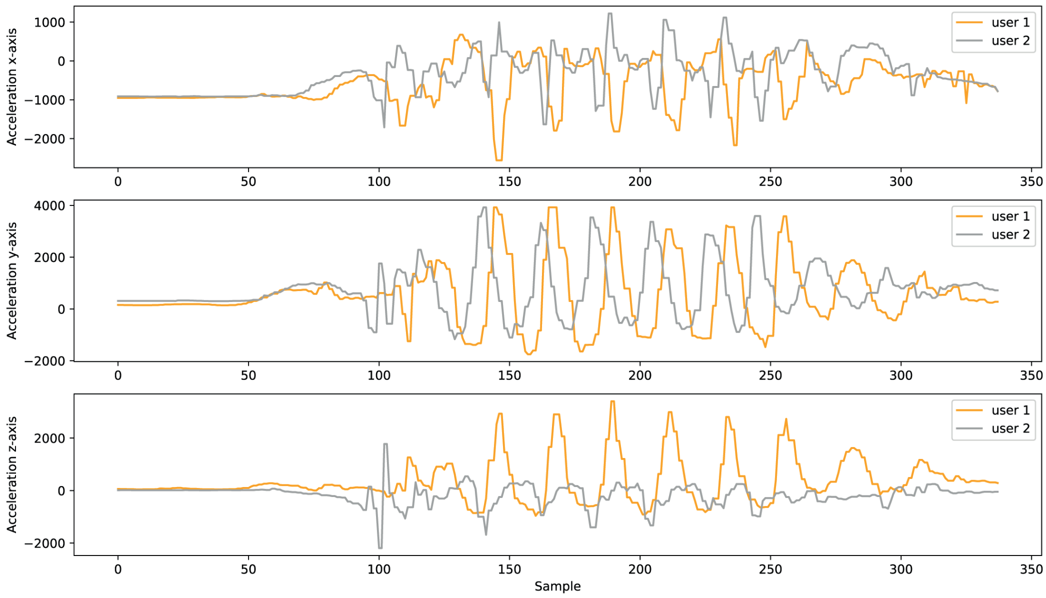

Figure 3.1: Plot of the acceleration signals for each axis of the corresponding handshake data. This data was recorded with a wrist-worn sensor at a sample rate of 75Hz. The acceleration is denoted in g*1000.

The raw acceleration data displayed in Figure 3.1 can be compared separately for each of the axes. Therefore, the raw sensor output provides three basic signals for a similarity comparison.

3.2.1 Composite signals

By combining the sample values of x, y, and z to a vector and calculating the length of it, one can obtain an aggregated signal. Consequently, the raw data can be used to create four composite signals $vxyz$, vxy, vxz and vyz see 3.2.

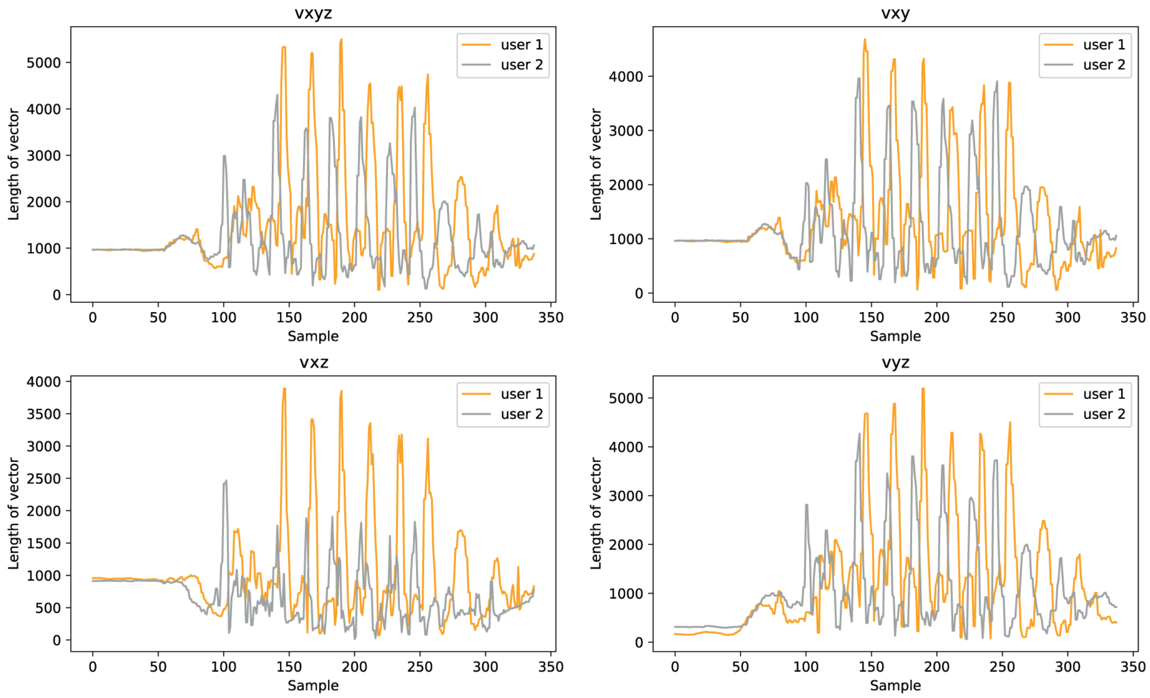

Figure 3.2: A plot of four corresponding composite signals. This data was recorded with a wrist-worn sensor at a sample rate of 75Hz.

3.2.2 Derived signals

Since acceleration is the rate of change of velocity at a specific moment, other physical values like the velocity or the covered distance can be calculated from it [15, p.9-11]. By computing these value transformations for the raw data and the composites, 14 additional comparable features are generated.

Velocity

By integrating over an acceleration signal, an accumulated velocity value for every sample point can be obtained.

$$v(n) = \int_{i=1}^{n} a(n)dn$$

The accumulated values were calculated with the *cumtrapz* function of the *scipy.integrate*[1] library.

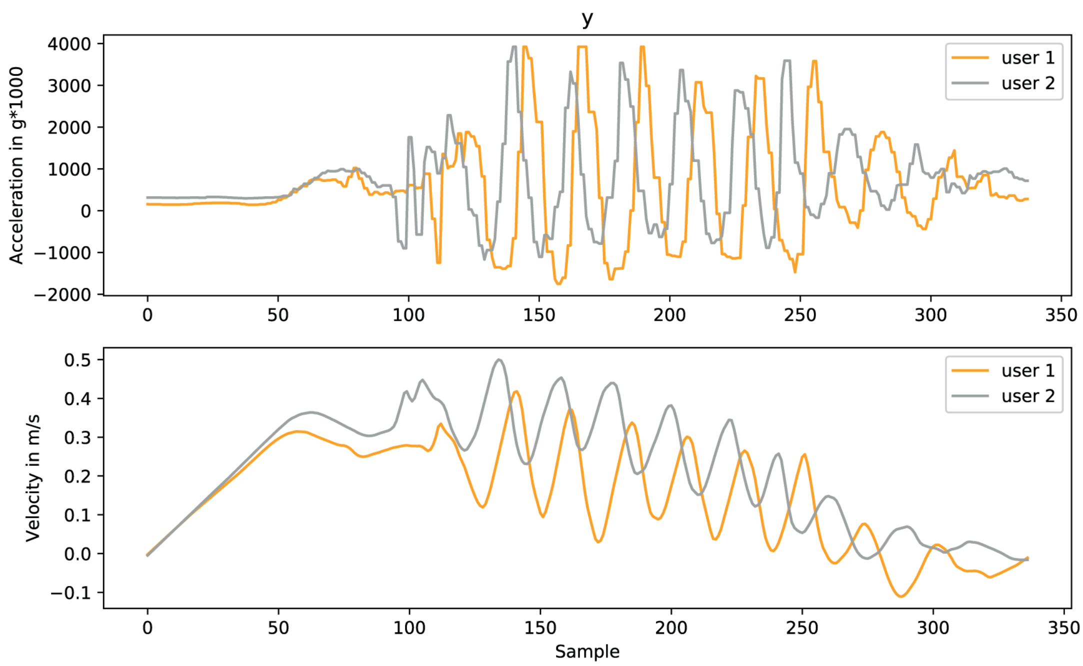

Figure 3.3: A plot of the accumulated velocity value at each sample point based on the raw y acceleration. This data was recorded with a wrist-worn sensor at a sample rate of 75Hz.

1 https://docs.scipy.org/doc/scipy/reference/generated/scipy.integrate.cumtrapz.html

Distance

With an additional integration of the velocity values, it is possible to compute a distance representation.

$$s(n) = \int_{i=1}^{n} v(n)dn$$

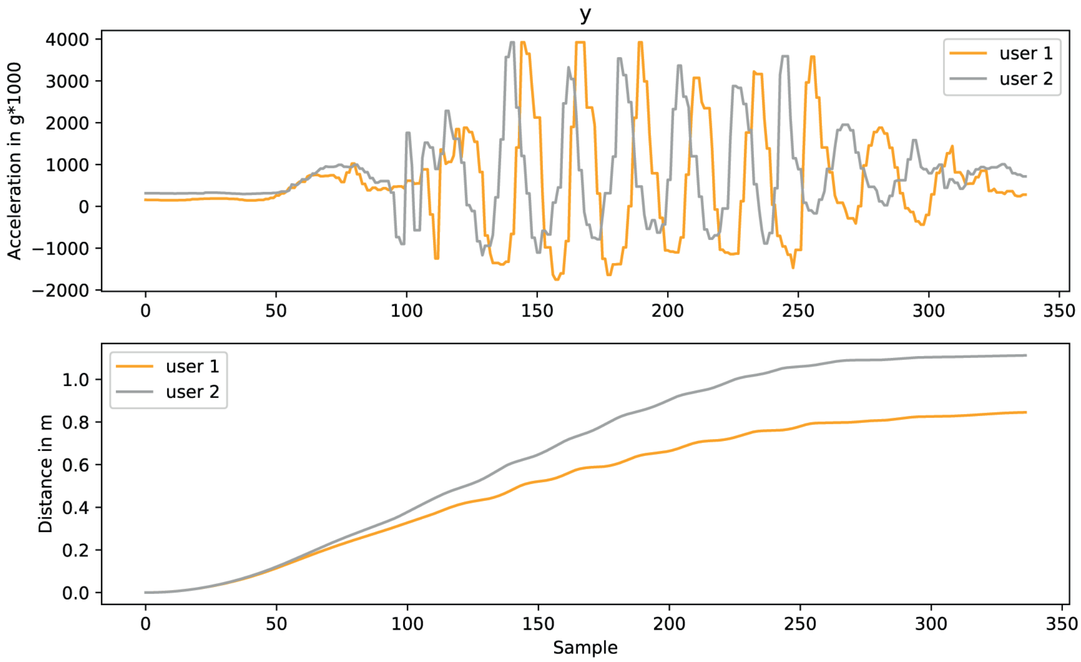

Figure 3.4: A plot of the accumulated distance values at each sample point based on the raw y acceleration. This data was recorded with a wrist worn sensor at a sample rate of 75Hz.

3.3 Challenges

During the exploration of several test recordings and the screening of related research, several basic problems were identified. Each of them influences and sometimes even aggravates the signal comparison.

3.3.1 Orientation mismatch

As shown in Figure 3.5 in a case of wrist deployed IMU the sensors are aligned. Due to their almost parallel alignment, the motion is registered on the respective axis of both sensors. Yet, in the case of a finger worn sensor, the orientation can be shifted. Therefore, the movement might be registered on a different axis or even be distributed over multiple axes.

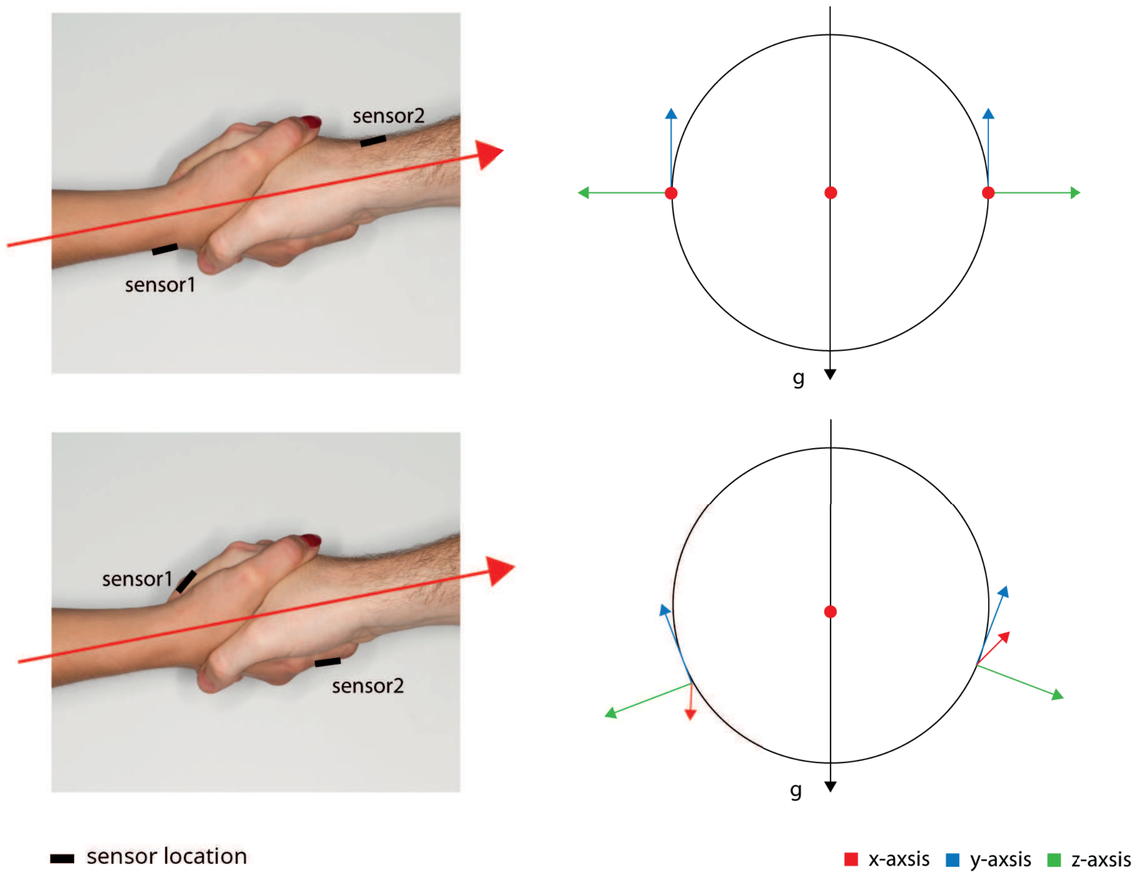

Figure 3.5: Explanatory visualization of the orientation mismatch.

This problem is amplified by the fact that an acceleration sensor is always influenced by Earth's gravity. Accordingly, one has to expect a nominal average acceleration value of 9.80665 m/s^2 that affects the different axis measurements depending on the sensor orientation. If both IMUs are properly aligned or are capable of filtering the influence of gravity, this effect can be neglected. Otherwise, it will induce a certain difference in the corresponding raw acceleration signals. However, the composite signal *vxyz* can be expected to be indifferent to the orientation mismatch since it is a representation of the assembled power of all three raw signals.

Besides, there is another circumstance that has to be considered when looking at the sensor orientations. Figure 3.5 also illustrates that if the sensors are oriented in the same manner, some axis might oppose each other. Consequently, they will produce inverted values. To prevent misinterpretation during the analysis the signals have to be preprocessed accordingly.

3.3.2 Time mismatch

Another problem is the time mismatch. When the two measurement units are not driven by the same clock, their output values can be shifted in time. In fact, this is very likely to happen in a scenario with independent mobile devices and when using split second measurement rates.

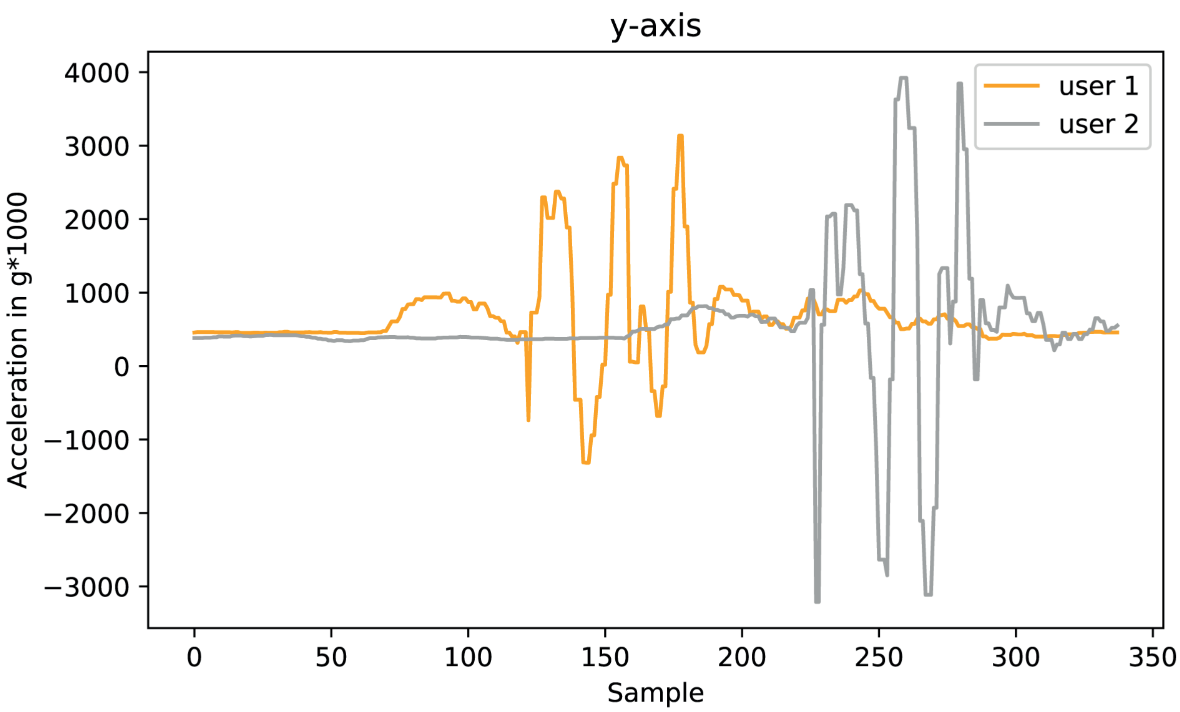

Figure 3.6: Plot of two corresponding y accelerations. The signals of the sensors are shifted in time.

3.3.3 Selection of a starting point

When comparing handshake motion signals with the intent to make use of their similarity, it is crucial to find a cohesive starting point. If the movement is embedded in a constant data stream, it is common to apply a sliding window approach combined with a classifier to discover the appointed motion in the signal [14]. Further possible strategies would be to use simple heuristics like amplitude thresholds or peaks [10]. It is also possible to deploy additional sensors [16] to detect the start of the synchronized motion phase.

3.3.4 Selection of a window size

Besides the selection of a starting point, it is important for a comparison to determine the end of a handshake motion. Handshakes can vary in length, but to avoid the inclusion of gesture unrelated data it is preferable to select the window size as small as possible. Melnyk[13] observed an average gesture duration of 2.67 seconds with a standard deviation of 0.86 seconds. In addition to that, Tange[16] and Wang[17] determined, that the physical contact phase of a handshake ranges somewhere between 0.65 seconds and 2.67 seconds.

3.4 Similarity criteria

To perform a detailed similarity comparison of the corresponding acceleration signals several criteria can be considered. An easy way to measure the similarity of two signals is to compare their amplitudes. Therefore, it is an established approach to calculate the correlation between them. Also, similar signals should display a recurrence of features. To prove resemblance one can test for several peak based values. Finally, there is the possibility to compute frequency based comparables from a signal.

3.4.1 Correlation

Usually, it is a straightforward way to express the coherence of two signals by combining all corresponding sample values.

$$\sum_{i=1}^{n} x_i * y_i$$

This generates a number that represents a relation between two signals. It is basically a value for the joint energy of the two signals. Nevertheless, due to the overall variations in amplitude of the different motion signals, this basic correlation is hard to compare. Therefore, it is necessary to create a normalized correlation (NC) by dividing it by a joint scaling factor.

$$\frac{\sum_{i=1}^{n} x_i * y_i}{\sqrt{\sum_{i=1}^{n} x_i^2 * \sum_{i=1}^{n} y_i^2}}$$

NC calculates a coefficient between -1 and 1 to express the relation of two signals. Thereby 1 is implying perfect coherence and -1 standing for inverse correlation. A similar measure of linear correlation is the pearson correlation (PC) coefficient also referred to as Pearson's r [18]. In principle, it is a normalized correlation but each value is diminished by the average energy of the signal. Pearson's r also calculates a value between -1 and 1.

$$\frac{\sum_{i=1}^{n} (x_i - \overline{x}) * (y_i - \overline{y})}{\sqrt{\sum_{i=1}^{n} (x_i - \overline{x})^2 * \sum_{i=1}^{n} (y_i - \overline{y})^2}}$$

As stated earlier correlation is based on the combination of time-corresponding sample values. Therefore it is susceptible to the time mismatch. A common approach in signal processing is to compute the cross correlation to determine if there is a lag between two signals. To calculate the cross correlation the signals are deferred stepwise while looking for the maximal correlation value. The total displacement between the position of the maximum correlation and the initial position is then interpreted as the time delay. After adjusting the samples of a signal to the lag, both the NC and the PC values can be considered as comparable features.

3.4.2 Points of interest

Further similarity criteria can be computed from the points of interest (POI). A POI can be a maximum, a minimum or a zero-crossing. As shown in related research [14] handshakes can be matched by comparing these POIs.

The simplest strategy to compare two signals with POIs would be to look at the peak counts. Obviously, this feature is very dependent on the peak detector and prone to signal noise. In fact, the peak count is often inaccurate. If used as a sole comparator it is very likely to match signals that do not belong together.

Another strategy is to examine if the positions of the detected POIs are aligned on the sample scale. If the corresponding signals are affected by a time mismatch, this will also lead to imprecise results. Consequently, for a reliable comparison, it would be necessary to compensate for an existing lag. If the delay is not too large as shown in Figure 3.7 it is possible to define an affinity range. Close maxima within that range could be interpreted as corresponding peaks.

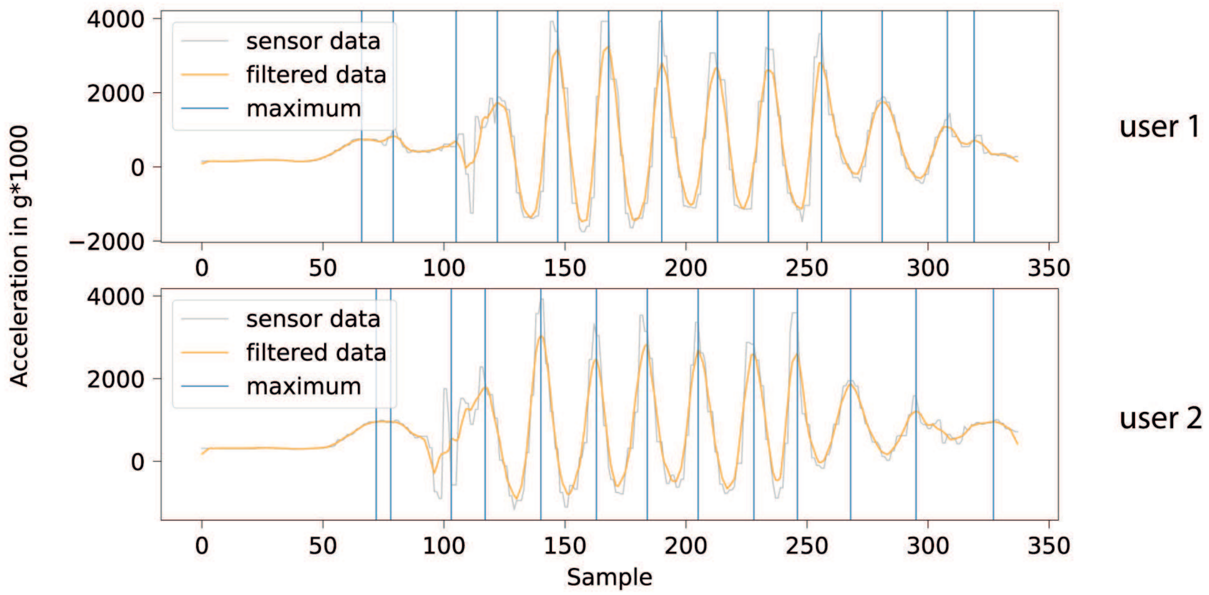

Figure 3.7: Plot of y acceleration maxima for two corresponding users. Before computing the peaks the signals were preprocessed to filter the noise. The total peak count for both users is 13. A slight delay is visible.

If both signals are based on the same sample rate, we can assume that the acquired acceleration signals are not warped in time. As a result, the distances between the POIs can as well be used as a similarity criterion. Given that the data is not too noisy or properly filtered, the distances between the peaks should be indifferent to the time delay. By computing the correlation of the distance values the peak distances can be used to express the similarity of two signals.

As suggested earlier, if the signals contain noise, the output of a peak detector can vary. Because of that, it is advised to smooth the signal and to filter the results either by thresholding or ranking. For instance, in case of a peak distance comparison based on maxima, it might be a good idea to only consider the five highest maxima of both signals.

3.4.3 Frequency analysis

It is a common approach to collate two signals by comparing the outputs of their Fast Fourier transformations (FFT) [19, p. 464 ff.].

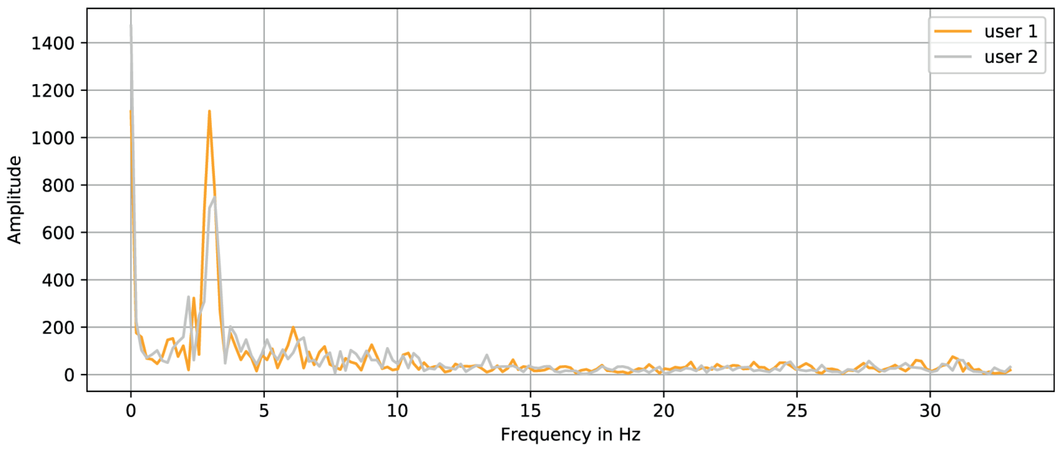

Figure 3.8: Frequency histogram for the corresponding y signals of Figure 3.1. The values were computed with the *fft()* function of the *scipy.fftpack* [1]library.

As a matter of fact, the correlation between the two FFTs is a good similarity criteria. Some of the handshake detectors are mainly based on the computation of this value [10]. Plainly, the FFT expresses a signal with sinusoids of varying frequencies. Hence, the algorithm

1 https://docs.scipy.org/doc/scipy/reference/fftpack.html

computes a representation of a signal in the frequency domain and returns a spectrum of frequencies cf. Figure 3.8.

Melnyk et al. [13] stated that the frequencies of a handshake gesture appear to be situated within the frequency band from 0 Hz to 10 Hz. They also identified 4.2 Hz as the main frequency that is dominant during the synchronized movement phase of a handshake. These findings coincide with the data acquired for this thesis.

3.5 Impact of preprocessing

It is possible to partially compensate for the effects of the previously mentioned mismatches by preprocessing the data. Hence, the measured similarity between two signals can be improved. Some of the methods described within this section have been applied in the later data analysis to improve the signal comparison.

3.5.1 Time shift adjustment

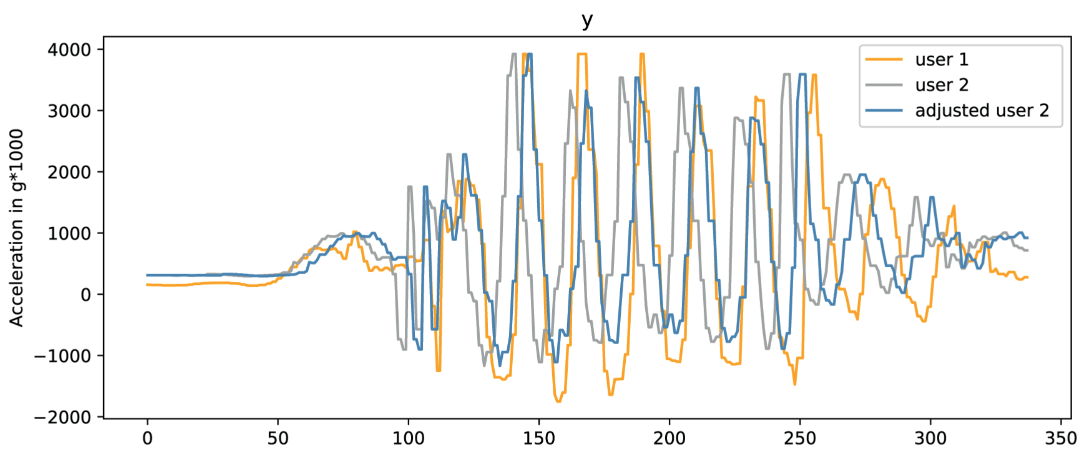

Figure 3.9: Plot of a y signal after applying the time shift adjustment.

By computing the cross-correlation mentioned in Section 3.4.1, the time mismatch can be determined. Before computing the different similarity criteria the signals have to be shifted by the delay while trimming or extending the ends of the signal by the shift to ensure an equal signal length cf. Figure 3.9.

3.5.2 Smoothing

To filter the noise from a signal it is common to apply a low-pass filter. A low pass filter can be applied by convolving a signal with a window of averaged sample values.

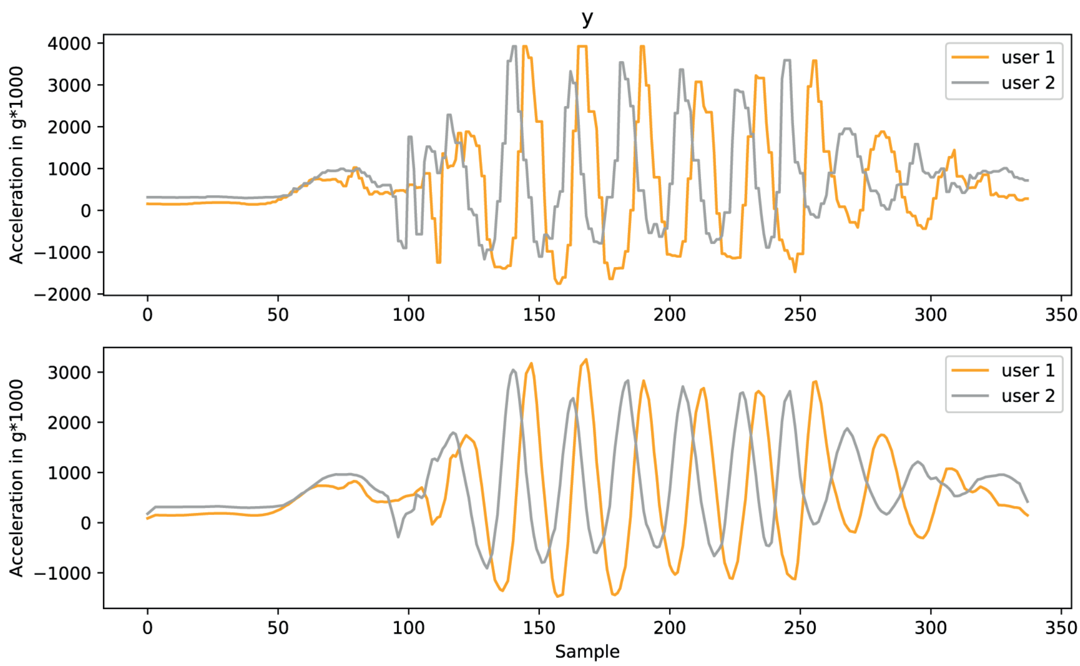

Figure 3.10: Plot of a y signal after convolving it with a seven sample average filter.

4 Measuring accelerations of handshakes

With the goal to acquire a dataset for the evaluation of sensor positions, a custom research setup was developed. The setup measured the motion at the wrist and the finger. It was composed out of two mountable acceleration sensors and a wearable processing unit. This chapter contains and documents the details of the setup to support replication and extension. First, Section 4.1 will discuss the hardware and Section 4.2 the deployed software. Section 4.3 presents the mounting solutions that were used to hold the hardware in place. Finally, Section 3.4 contains some information on the latency and transfer rates of the setup.

4.1 Hardware

The system was built with of-the-shelf hardware and development boards. For the purpose of further development, all the different components were selected to be built into a custom printed circuit board (PCB). Each measuring unit consisted out of two sensor units and one microcontroller with Bluetooth capabilities. To make the process of data acquisition more flexible the system was designed to be portable. Therefore, the controlling hardware was placed into mountable pockets.

The motion sensor used in this setup was the BNO055 [20]. This Inertial Measurement Unit (IMU) contains a magnetometer, a gyroscope, and an accelerometer. To lower transmission load and to generate results comparable to previous research, only the acceleration data is recorded and processed. During the course of this thesis, the sensor was mounted on a breakout board to speed up the process of building the system and to ensure easy access to the contact pins of the IMU.

The green and yellow connections in Figure 4.1 show that the BNO055 was connected to a nRF52 microcontroller via an Inter-Integrated circuit (I^2C). This microcontroller fulfilled the tasks of retrieving and forwarding the acceleration data. It was selected because of its built-in BLE capabilities. Hence, there was no need for a supplementary BLE unit.

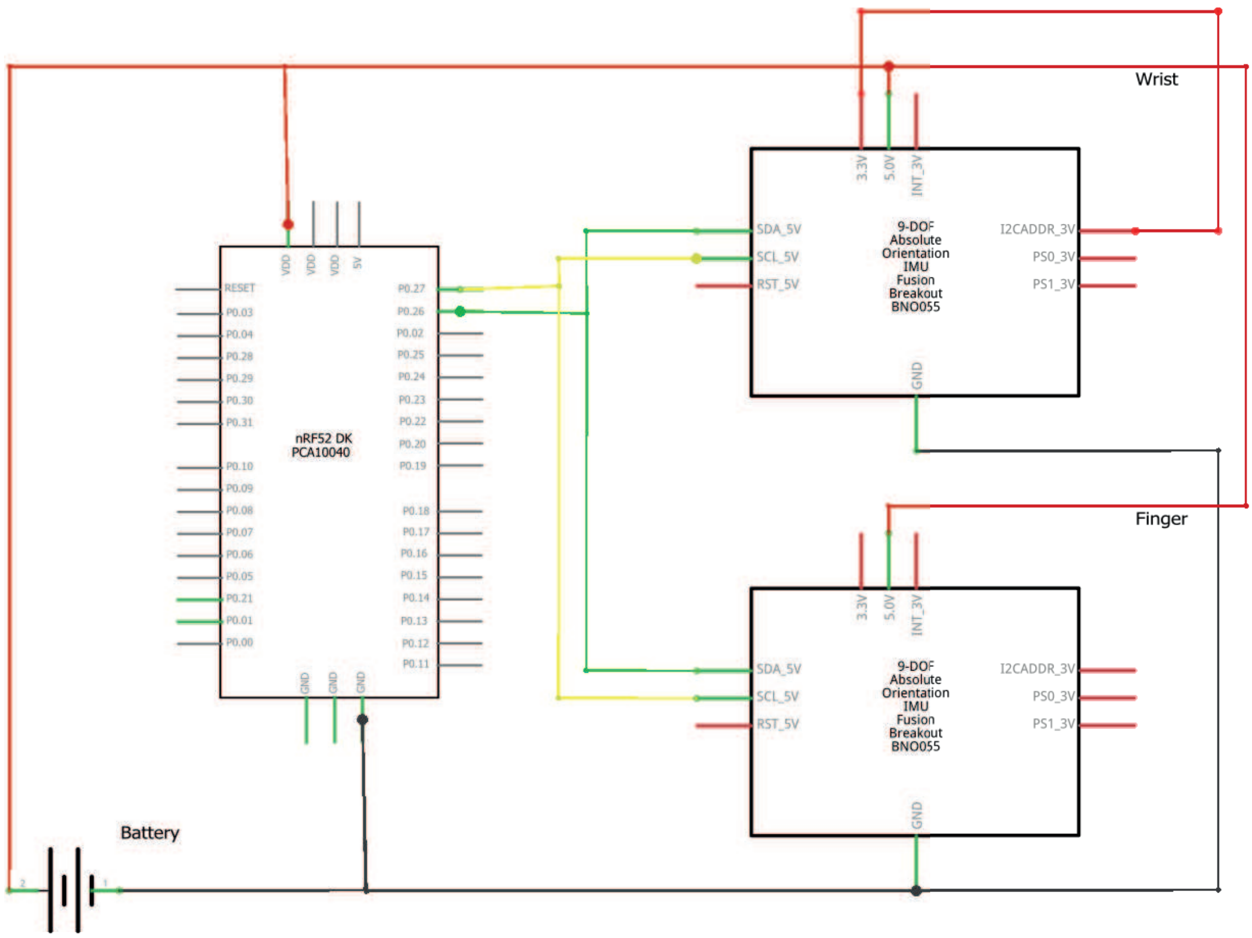

Figure 4.1: Circuit layout of the gathering units. Each unit contained two IMUs and one microcontroller. This graphic was created with fritzing[1].

Especially, when considering the development of a custom PCB, this feature would save some space on a custom board. Although, for this particular gathering setup the nRF52 was still mounted on the development board to speed up re-programming and to have easy access to the necessary pins.

During each recording session, the data was transferred by the nRF52 to a respective Android smartphone via BLE. The phone model used for the data acquisition was the Nexus 5[2] running Android 6.0.1. To improve the transmission rate, each gathering unit was coupled with another identical Android device.

1 http://fritzing.org/download/
2 https://support.google.com/nexus/answer/6102470?hl=en

The mobile measurement units were powered by 52540 lithium batteries. This rechargeable battery has a capacity of 680 mAh and an output voltage of 3.7 V. This power source was sufficient to supply the setup for several days with multiple recordings.

4.2 Software

As mentioned in the previous section, the setup is based on two different processing units. The programs for the nRF52 were developed in C utilizing the nRF52 SDK v12.2.0, while the corresponding Android application was programmed in Java. Figure 4.2 shows the different modules that were built for this setup. Additionally, it displays the involved drivers and interfaces.

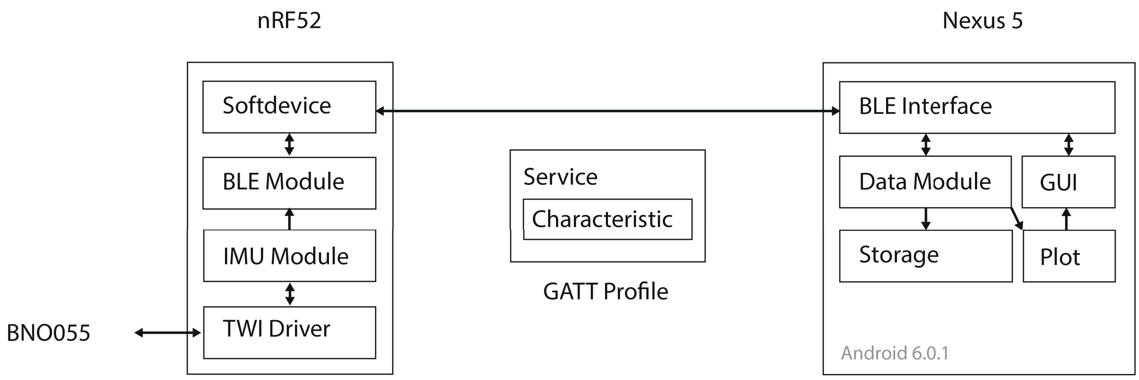

Figure 4.2: Overview of the deployed modules and the basic software structure.

The communication between the microcontroller and the IMU was accomplished via an I^2C bus. Nordic, the manufacturer of the nRF52, supports the I^2C standard with a custom driver. Within their documentation, it is referenced as a two-wire interface (TWI). The TWI provides several functions to initiate the connection or to manage the data transfer. These functions were called upon in the IMU module. It maintained the bus connection and surveyed the accelerometer data from the BNO055.

Another program that ran on the microcontroller is the BLE module. It fulfilled the task of handling the connection between the nRF52 and the Android device. Almost all of the Bluetooth capabilities of the nRF52 can be accessed via the so called Softdevice. The Softdevice contains a driver for the BLE capabilities of the microcontroller and provides an interface to access the functions compliant with the Bluetooth standard. To simplify further development, the sensor data was stored in a Generic Attribute Profile (GATT). This concept is used within the BLE standard to streamline the way data is structured and sent back and forth. GATT organizes data in Services and Characteristics, which can be accessed after a connection is established between two BLE devices. Also, according to the BLE standard, the nRF52 was set to work as a peripheral device.

To facilitate the process of data gathering, the smartphone was designated to work as a central device. Therefore, the application had built-in functions to scan for BLE supporting sensor modules and to initiate and maintain a BLE connection. Within Android, most of the BLE traffic was administered through an event interface. Furthermore, the application had the functionality to start a timed recording session by the press of a button. Additionally, it displayed a plot of the received data and stored it in the *Download* folder of the Android device. All of these functions were accessible through a basic graphical interface in the app.

4.3 Mounting

When considering mounting solutions, the first requirement was to have a size-adjustable setup that fits participants with different physiological properties. Additionally, the process of gearing up should not be complicated and not take too much time. Finally, the gathering setup should be mobile since it was supposed to be deployable outside of a laboratory.

To match these requirements, the development board and the power supply were stowed in a small bag. This kind of bag is usually used to carry a smartphone during sports and outdoor activities. Hence, it could easily be mounted on the arm of a participant with an attached velcro band. As displayed in Figure 4.3, it was always wrapped around the upper arm of a person.

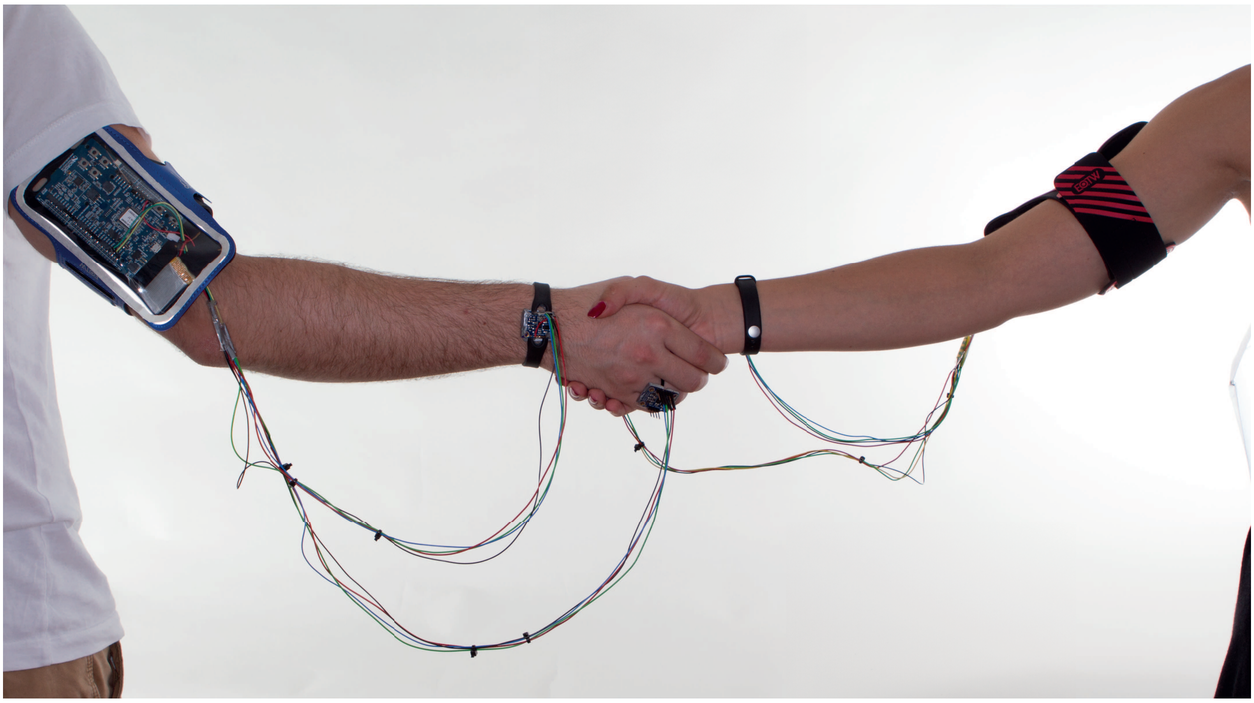

Figure 4.3: Photograph of a handshake with both participants wearing the data gathering gear.

At this position, the bag was less disturbing for the wearer and its influence on the movement during a handshake was reduced. Furthermore, the wrist sensor was glued to an adjustable wristband that normally works as a holder for the MIBand [1] hardware. The finger sensor was fixed to a cable tie loop that could be fastened and loosen.

4.4 BLE transfer and sample rate

The BNO055 supports sampling rates up to 1000 Hz. In this setup, the IMU was set to operate at a rate of 125 Hz instead of the default 62.5 Hz [20]. This frequency was selected because it was closest to the sample rate of 100 Hz which was used during the Shakecast project [10]. To ensure seamless data throughput to the microcontroller, the I^2C bus was configured to run at the highest possible frequency of 400 kHz. The BLE settings of the nRF52 were left at the default values of the SDK examples. To reduce the BLE traffic, the GATT characteristic was set up to use BLE notifications. Since notifications do not

1 http://www.mi.com/en/miband/

need to be acknowledged they are more suitable to ensure a steady data stream from the peripheral to the central device.

Based on the specifications, BLE [21] is supposed to provide enough throughput to transfer the measures provided by the IMU. In Android 6.0.1 the Bluetooth stack is set to work at a minimal connection interval of 11.25 ms. Additionally, the transferred data fitted in the 20 byte payload of one BLE package, while leaving 6 bytes unused. Also, the system was set to establish a new connection to the peripheral device each time the recording was triggered manually. Consequently, each recording had a connecting period in the beginning where no acceleration data was transferred.

However, during development the best sample rates that could be achieved with the Nexus 5 ranged around 70 Hz. In detail, this means that during a recording period of 6 seconds 420 acceleration values were registered on the Android device. In comparison, when testing the system with a OnePlus 2[1] sampling rates around 133 Hz were obtained. It is likely that the reason for this gap is the difference in the supported Bluetooth standards. The Nexus 5 supports the older Bluetooth 4.0 while the OnePlus 2 supports the newer Bluetooth 4.1 standard. Although, it was not determined which part or setting within the Bluetooth stack caused this discrepancy. To provide comparable rates for different devices an update timer was built into the BLE characteristic of the nRF52 and set to 10 ms.

Overall the gathering setup worked with an average sampling rate of 66,43 Hz. This value was computed by averaging the sample rates of 90 datasets that were recorded during the data acquisition described in Chapter 4. In order to map the movements of a handshake this sampling rate was sufficient.

1 https://oneplus.net/de/2/specs

5 Acquisition process and the dataset

The previously described hardware was used to gather two distinct datasets. Since the system was designed to be mobile, some of the recording sessions were conducted outside of a laboratory environment. Each session followed a predefined procedure which is described in Section 5.1. The following Section 5.2 describes the metrics and properties of the two recorded dataset.

5.1 Data gathering procedure

To gather a comparable dataset a sequence plan was developed and used during the acquisition of each dataset. A recording session took between 7 and 15 minutes. It started with a short introduction about the reasons and ideas behind this thesis and the purpose of the participants data being collected. In the next phase, the sensors and the transmitter were mounted to the right arms of both participants. While informing the participant's about the procedure and reminding them to refrain from exaggerated gestures, the power was switched on and a short connection test was executed. When the test was successful both participants were positioned facing each other.

After the introduction, the experimenter started both recordings by pressing a button on the coupled smartphones while verbally signaling the participants to start the gesture. After six seconds the recording was automatically terminated and the experimenter reviewed the signal plots on each phone. In case a plot was indicating a sensor or transmission failure an additional iteration of the recording sequence was performed. This procedure was repeated till five to seven gestures were recorded.

To complete the session every attendee had to fill out a data release form and received a small symbolic reward for the participation.

During the whole gathering process three mentionable observations were made:

a) *Many participants started to smile during the recording and expressed bashfulness in their body language.*

b) *Some participants mentioned that they touched the acceleration sensor on the finger of their partner during the handshake.*

c) *In three cases a participant told the experimenter, that the finger mount had loosened during the gesture.*

5.2 Dataset structure and metrics

The dataset includes a total of 90 handshakes. During the acquisition process, 60 people participated in pairs. Hence, the set consists of 30 unique pairings. This structure was selected to diminish the possibility that dominant shakers would influence the dataset more than others and to create unique handshakes. To reduce the influence of outliers within a recording session, each pairing contributed three selected handshakes. The other recordings were discarded. Therefore the dataset contains a total of 90 handshake samples. Each sample consists of four recordings containing the data of the four respective sensors. The majority of the participants were acquired in a university environment. Since the participants were not surveyed there is no verified demographic information available.

The data was structured in serially numbered folders. The parent folder represents the pairing and contains subfolders, named "user1" and "user2". Within these subfolders the acceleration data was stored in comma-separated value (CSV) files. All files that contain a "A" in their filename belong to a sensor located on the wrist of a participant while all files labeled with a "B" hold data from a finger sensor.

When evaluating the dataset an average of 398.38 datapoints per sensor file was calculated. The lowest point count is 338 and the highest 422. This difference is probably based on packaged loss of the BLE connection.

6 Data analysis and evaluation of sensor locations

To conduct a thorough examination of the dataset a custom tool was developed. This program as described in Section 6.1 was used to compute the similarity measures and to aggregate the results. In Section 6.2 the different similarity tests are evaluated. Additionally, a representative similarity test is selected for the final comparison of the sensor locations. Subsequently, the analysis of the selected similarity criteria is done in Section 6.3. It also holds the concluding results of this comparison and discusses the observations in the context of other valid similarity tests.

6.1 Analysis tool

The analysis program was developed in Python. This programming language was selected due to its extensive data evaluation libraries. Accordingly, the developed tool was used to calculate multiple similarity measures from the corresponding finger and wrist sensors. These measures were computed by matching wrist data to wrist data and finger data to finger data.

6.1.1 Program structure

The tool was structured in the main module, the comparator and the generator. When the tool was started, the main module initiated the loader and administered the signal comparisons. Furthermore, it managed the generation of the statistical evaluations. After a call from the main module, the loader script parsed the data from the CSV files of the dataset into a simple object based data structure cf. Figure 6.1.

Afterwards, the data for the corresponding sensor pairs was forwarded into the comparator. This class returned a matrix with the results of the conducted similarity tests.

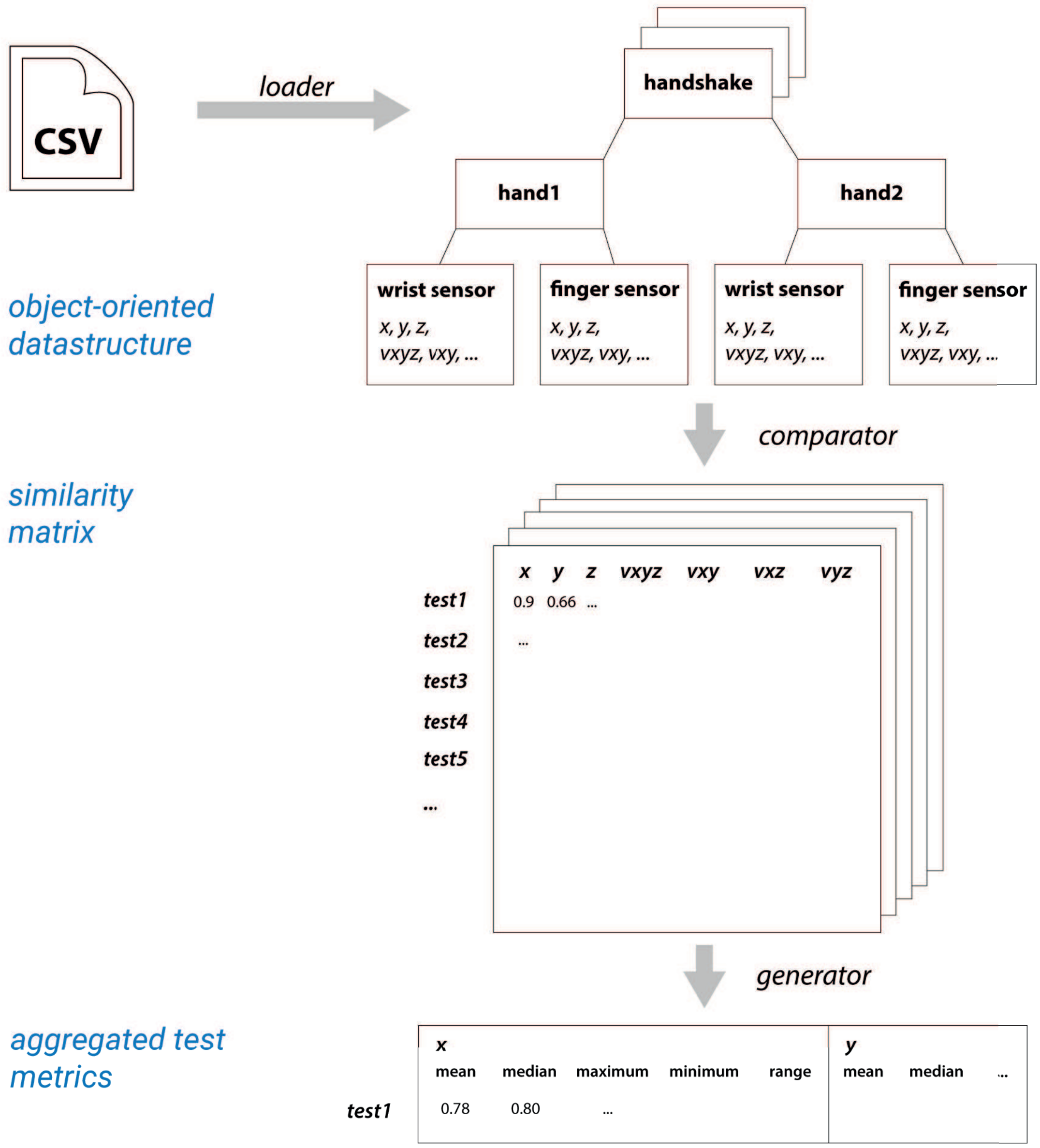

Figure 6.1: Information processing queue in the analysis tool.

The output matrices were combined to a three dimensional array to create a representation for the complete dataset. Finally, this new array was used to compute the aggregated metrics for example the mean or the median correlation values for every similarity tests.

6.1.2 Similarity tests

Based on the correlation coefficients discussed in Section 3.4.1 a series of comparative functions were implemented into the comparator module. All of them were applied to the different raw and composite acceleration signals. Additionally, the module contains two functions to compute a similarity test for the derived velocity and distance values.

- **The normalized correlation** was computed with the formula described in Section 3.4.1. The acceleration signals were preprocessed with a timeshift adjustment based on the cross-correlation of *vxyz*. This adjustment was capped at 50 samples.
- **The Pearson's correlation** was computed with the formula described in Section 3.4.1. The acceleration signals were preprocessed with a timeshift adjustment based on the cross-correlation of *vxyz*. This adjustment was capped at 50 samples.
- **The peak distance Pearson's correlation (maxima)** was computed by calculating the Pearson's correlation of the distances between the maxima of two signals. To filter the noise and improve the peak detection the signals were preprocessed with an averaged convolution. The peak detection was done with a *detect_peaks()* function ported from matlab.
- **The peak distance Pearson's correlation (minima)** was computed by calculating the Pearson's correlation of the distances between the minima of two signals. To filter the noise and improve the peak detection the signals were preprocessed with an averaged convolution. The peak detection was done with a *detect_peaks()* function ported from matlab.
- **The FFT Pearson's correlation** is based on a Pearson's correlation of the FFT values in a range from 2 samples to 35 samples. The FFT was computed with the *fft()* function of the *scipy.fftpack* library.
- **The velocity Pearson's correlation** is based on a Pearson's correlation between the derived velocity values cf. Section 3.2.. The signal was preprocessed with a timeshift adjustment based on the cross-correlation of *vxyz*. This adjustment was capped at 50 samples. The correlation value was computed with a Pearson's correlation coefficient.

- **The distance Pearson's correlation** is based on a Pearson's correlation between the derived distance values cf. Section 3.2. The signal was preprocessed with a timeshift adjustment based on the cross-correlation of *vxyz*. This adjustment was capped at 50 samples. The correlation value was computed with a Pearson's correlation coefficient.

A table with the aggregated results of these different comparisons can be found in the appendix.

6.2 Evaluation and selection of comparative tests

All of the aforementioned similarity tests were supposed to be consulted in the final analysis. The tests were evaluated by reviewing the range, the median and the mean of the correlation values. Each of these aggregated metrics was computed for every raw (*x,y,z*) signal and every composite (*vxyz,vxy,vxz,vyz*) signal. Furthermore, the maximal and the minimal correlation value of the aggregated comparisons were examined. Additionally, plots of the correlation distributions were reviewed.

In order to have a point of reference, a control set was generated from the dataset. In this set, the correlations were computed with non-corresponding motion signals. By pairing each hand object with partners from different recordings a new list of mismatched handshakes was created. Since every object was combined with all possible not matching partners. Based on a set of 90 matched handshakes, the generated control set reached a size of 8010 falsely matched handshakes. The aggregated metrics for each sensor location can be reviewed in the appendix A.1 and A.2.

6.2.1 Disqualified similarity tests

While looking at the metrics it became obvious, that the peak based similarity tests for minima and maxima did not return very reliable values for a comparison. In general, they produced correlation values in a range from 0.1 to 1 with a median and a mean correlation value around 0.7. However, the tests returned only slightly lower values for the control set. The difference between the mean and median correlation values of the data set and the control set was below 0.1. In comparison, the differences for the other tests ranged around 0.2 or even 0.3 depending on the compared signal.

This indicates, that the peak detection in its current form needs some further adjustments for the peak distances to work as a good similarity measure. This test relies heavily on the detectors ability to find and return the same peaks in the compared signals. Another factor that might have an impact on the results is the sample rate of the signals. Given a set of handshakes with a fast up and down movement and a low sample rate, the computation of the peak distances will only return values in a small range. Hence, it is more likely that they will return similar peak distances. This might be the reason for the high correlation values of the control set. Consequently, it disqualifies the applied peak distances as a convincing similarity test. It is also debatable if Pearson's R is the right similarity coefficient when the peak distances turn out to be very similar.

A similar lack of variety was observed for the distance correlation test. The test returned an average mean and median correlation of around 0.97. This was observed for the set of truly matching handshakes as well as for the mismatched set. Again the difference in mean and median correlation between the two sets was below 0.1 for all compared signals. Undoubtedly, these control set values disqualify the distance correlation as a similarity measure to compare the sensor locations. Yet, they also suggest that the overall distance a hand moves during a handshake is similar for all the recorded handshakes.

Finally, the normalized correlation suffered from the same problem. The difference in mean and median correlation between the dataset and the control set was below 0.1 for all signals except for the y signal. Accordingly, this is shows that the normalized correlation does not perform very well when comparing the signal data of a handshake.

6.2.2 Selection of comparable similarity tests

The remaining three similarity tests produced rather equal results. During the comparison with the control set their mean and median values deviated in average by 0.22. When reviewing the aggregated metrics of each of the three tests, it was not possible to determine if one of them performed better than the other. Therefore, the FFT Pearson's correlation (FFTPC), the velocity Pearson's correlation (VPC) and the Pearson's correlation coefficient (PCC) are considered valid similarity tests for the following evaluation.

6.3 Signalwise comparison of sensor locations

The main evaluation of the sensor location was conducted with the results of the FFT based similarity test. This test was selected because its closer tie to the previous research of the Shakecast project. However, the following statistical tests were computed for each of the three selected similarity tests. Accordingly, the results can be reviewed in the appendix A.3 and A.4. To avoid repetitive argumentation during the signal analysis only deviations between the tests will be discussed for each signal. Afterwards, a short performance comparison of the two sensor location is conducted with the test results.

6.3.1 Evaluation approach and applied statistical methods

As stated earlier the similarity tests provided a correlation value for every handshake of the dataset. Therefore, each similarity test returned a set of 90 varying correlation values. These value distributions were compared for the finger and the wrist sensor to ascertain which sensor location provided a signal of better resemblance.

The applied statistical procedures and methods were selected from Andy Field's textbook about statistics [22]. The actual statistical tests were computed with a python program utilizing the respective statistical functions form the *scipy.stats* library [23].

At first, the correlation distributions were analyzed for normality with the Shapiro-Wilk test [24]. This test can be used to examine if the values of a distribution are normally distributed. The confidence interval for this test was set to an $\alpha = 0.05$.

Shapiro-Wilk test:
H_0: One sample is drawn from a normally-distributed population.

H_1: One sample is not drawn from a normally-distributed populations.

Nevertheless, for uncertain p-values the QQ-plots of the compared distributions were consulted. Afterwards, a second statistical test was conducted to check if the distributions were significantly different. In the case of a non-normal distribution, the Wilcoxon signed-rank test [25] is a useful tool to provide further information about two dependent distributions. Whereas, if the data turned out to be normally distributed a paired t-test can be applied. Both these tests are used to determine if there is a significant difference between the two sensor locations.

Wilcoxon signed-rank and paired t-test:
H_0: There is no difference between the correlation values of the two sensor locations.

H_1: There is a difference between the correlation values of the two sensor locations.

However, especially the Wilcoxon signed-rank test only reveals the existence or the absence of a significant difference between two value distributions. Besides, it should be noted, that the Wilcoxon test function from the scipy.stats library only returns the smaller one of both w-statistics and the computed p-value. To provide comparable statistical results, the z-score and the effect size r were computed with formulas derived from Andy Field's book [22, p227-237]. Both values can be computed with sample size dependent standard error σ.

$$\sigma_w = \sqrt{\frac{N * (N+1) * (2 * N + 1)}{24}}$$

$$z = \frac{W - \overline{W}}{\sigma_w}$$

$$r = z/\sqrt{N}$$

With N=90 being the number of sample values a $\sigma_w \approx 248,52$ and a $\overline{W} \approx 2047,5$ were computed. These values were used to compute the z-score and the effect size for the smaller w-statistic returned by the Wilcoxon signed-rank test. Obviously, without knowing which sensor is represented by this w-statistic, the effect size can only be used to inform about the magnitude of the effect, not the direction. Therefore, in the case of a non-normal distribution the median difference and the computed effect size were consulted to provide a statement about the performance of a sensor location. The effect sizes r of the Wilcoxon signed-rank tests were rated according to Cohen's r increments 0.1, 0.3 and 0.5 [26].

With H_0 and H_1 as an underlying hypothesis for the paired t-test and the Wilcoxon signed-rank test, the confidence interval α was set to *0.05*. This leaves a 5% chance that the statistical tests detects a significant difference if there is none.

6.3.2 x, y, z signals

At first, correlation values of the FFT were tested against a normal distribution with the Shapiro-Wilk test. For the raw x-axis acceleration signal the test returned a p-value of 0,057591 for the finger sensor and a p-value of 0,471413 for the wrist sensor. Based on the $\alpha = 0.05$ assumption it can be conducted that both datasets are normally distributed. However, since the p-value of the finger sensor was rather close to the threshold, the QQ-plots of both distributions were consulted.

As displayed in Figure 6.2, the correlation distributions deviate from the normal distribution and show a slight skew. For this reason, the normality assumption was neglected and the non-parametric Wilcoxon signed-rank test was applied.

Wilcoxon signed-rank test based on FFT correlation values (*x-axis*):

w-statistic = 1653, *p-value* = 0,11243
z-score(w_{min}) = -1,58740, *r*(w_{min}) = -0,16733
$Median_f - Median_w$ = -0,16267

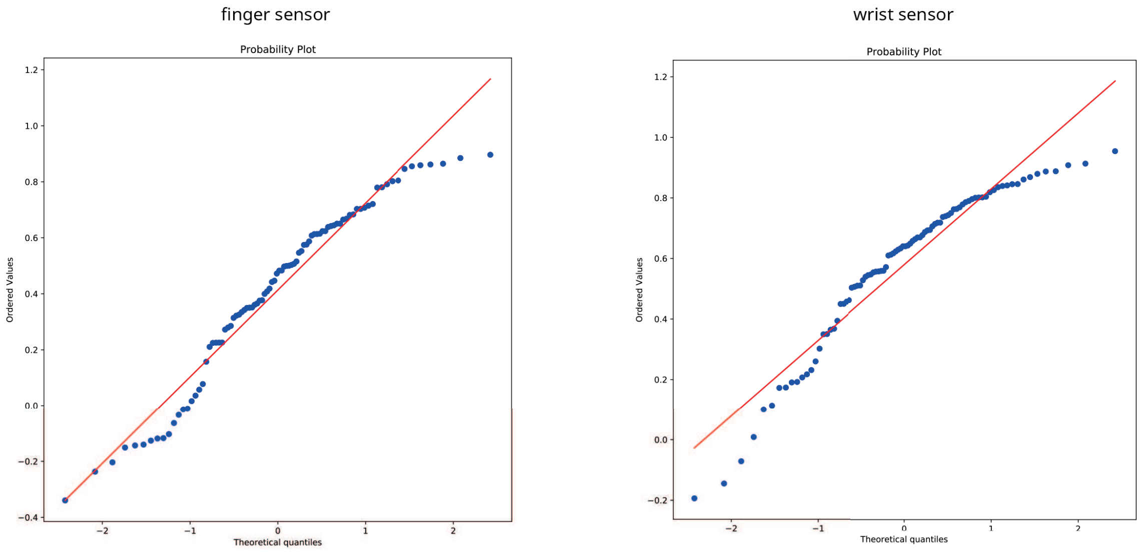

Figure 6.2: QQ-plot of the finger and the wrist based FFT correlation distributions.

As displayed above the test returned a p-value of 0,11243. Unquestionably, this value is higher than the selected α. Accordingly, H_0 can not be rejected and no significant difference between both distributions were detected. However, an effect size r of -0,16733 indicates a small effect when compared to Cohen's increments. This suggests that there might be an effect that can not be proven with the current number of samples. By reviewing the results of the Shapiro-Wilk test for the PCC and the VPC values, the distribution determined as non-normal for both of them. Consequently, the Wilcoxon signed-rank test was applied. In contrast to the FFTPC, their distributions were significantly different. Furthermore, large effect-sizes above 0.5 were computed. The median difference between the wrist correlation values and the finger based correlation values showed, that the sensor on the wrist produced acceleration values of higher similarity.

The next FFTPC values, were computed with the y-axis acceleration. This time, the Shapiro-Wilk test returned a p-value smaller than 0.001 for the finger and the wrist data. Hence, it was below the α threshold. Consequently, the correlation values were not normally distributed and the Wilcoxon signed-rank test was used to compare the sensor locations.

Wilcoxon signed-rank test based on FFT correlation values (*y-axis*):

$$w\text{-}statistic = 558,\ p\text{-}value = 0{,}00001$$
$$z\text{-}score(w_{min}) = -5{,}99348,\ r(w_{min}) = -0{,}63177$$
$$Median_f - Median_w = -0{,}32131$$

With a p-value below the α of 0.05 H_0 can be rejected. Hence, the Wilcoxon signed-rank test indicates that there is a significant difference between the wrist and the finger FFTPC values. An effect-size of r = -0,63177 arguments for large effect of the location on these values. Besides the median difference of -0,32131 is a strong indicator, that the wrist signals had a greater resemblance than the finger signals. This result was matched by the other two similarity tests. They also returned large effect sizes and a better performance of the wrist sensor.

The FFTPC was also applied on the z-axis data. This time the Shapiro-Wilk test returned a p-value = 0,00001 for the finger based distribution and a p-value = 0,25551 for the wrist based distribution. In contrast to the wrist correlation values the finger correlation values were not normally distributed. Therefore the paired t-test was not applicable and the non-parametric Wilcoxon signed-rank test was used.

Wilcoxon signed-rank test based on FFT correlation values (*z-axis*):

$$w\text{-}statistic = 1180,\ p\text{-}value = 0{,}00048$$
$$z\text{-}score(w_{min}) = -3{,}49066,\ r(w_{min}) = -0{,}36795$$
$$Median_f - Median_w = 0{,}14193$$

A p-value of 0,00048 indicates a significant difference between the two distributions and allows a rejection of H_0. Although, this time the median difference states that the finger correlation values have a greater resemblance than the wrist based values. With an effect size above the 0.3 increment a difference of medium magnitude is indicated. Hence, it can be deduced that the sensor located on the finger performed significantly better than the wrist located sensor on the z-axis data. Since not normally distributed, once again the PCC and the VPC test values were examined with the Wilcoxon signed-rank test. Their median difference aligns, with the bias towards the finger based sensor values. However, the test only returned a p-value of 0,173192 for the VPC. This value is above the α of 0.05. Therefore, for the velocity based distributions, H_0 could not be rejected and no significant difference can be assumed. In comparison to the PCC distribution it also only displayed a small effect with an effect size of -0,14357.

6.3.3 vxyz and other composites

According to the procedure for the raw acceleration signals, the composites were also used for a statistical evaluation. The first test was done with the *vxyz* signal. When examined with the Shapiro-Wilk test the FFTPC distributions returned a p-value below 0.00001. Again, this allowed the assumption of a non-normal distribution in both cases.

Wilcoxon signed-rank test based on FFT correlation values (*vxyz*):

$$\textit{w-statistic} = 1812, \textit{p-value} = 0{,}34334$$
$$\textit{z-score}(w_{min}) = \text{-}0{,}94761, r(w_{min}) = \text{-}0{,}09989$$
$$Median_f - Median_w = \text{-}0{,}09546$$

However, the FFTPC produced a p-value of 0,34334 in the Wilcoxon signed-rank test. Because of that, H_0 could not be rejected and no significant difference between the two distributions was presumed. Another observation that coincides with this result is the small median difference. Furthermore, an effect-size below the 0.1 increment suggests that no conclusions can be drawn from this correlation distribution. The PCC and the VPC distributions were although examined with the Wilcoxon signed-rank test. Although, their p-values indicated a significant difference between the wrist and the finger based sensor data. In fact, their median difference of 0,04803 for the Pearson correlation test and 0,02009 for the velocity correlation test imply a better performance of the sensor located at the finger. Admittedly, the median differences were relatively small. However, this assumption is strengthened by a medium effect-size. In fact, the low median differences were observed with most tests for z-axis related composites.

Especially for the FFTPC values of the vxz composite. Again, the distributions of the FFTPC were found non-normal with the acquainted test and analysed with the Wilcoxon signed-rank test.

Wilcoxon signed-rank test based on FFT correlation values (*vxz*):

$$\textit{w-statistic} = 1206, \textit{p-value} = 0{,}00071$$
$$\textit{z-score}(w_{min}) = \text{-}3{,}38605, r(w_{min}) = \text{-}0{,}35692$$
$$Median_f - Median_w = \text{-}0{,}00945$$

The test returned a medium effect size and a p-value below the selected confidence interval. Therefore, a significant difference can be assumed. The VPC distributions showed a significant difference between the finger and the wrist data for *vxz*. Whereas, this time no difference was detectable between the PCC distributions.

Another z axis related composite is the vyz signal. Again, the Shapiro-Wilk test imputed a non-normal distribution. Accordingly, the FFTPC distributions were analysed with the Wilcoxon signed-rank test.

Wilcoxon signed-rank test based on FFT correlation values (*vyz*):

$$\textit{w-statistic} = 1853,\ \textit{p-value} = 0{,}43386$$
$$\textit{z-score}(w_{min}) = -0{,}78263,\ r(w_{min}) = -0{,}08250$$
$$Median_f - Median_w = 0{,}02691$$

With a p-value ¿ α the null hypothesis was not rejected. Consequently, no significant difference was detected between the distributions of the wrist and finger derived values of the FFTPC. In contrast, the Wilcoxon signed-rank test returned different results for the PCC based similarity test. The VPC test distribution also provided different results. Both similarity tests indicated a significantly better performance of the wrist sensor.

Finally, the vxy composite was examined. When computing the Shapiro-Wilk test for the FFTPC distributions, the test returned a p-value below 0.00. Therefore, the FFTPC values were also not normally distributed.

Wilcoxon signed-rank test based on FFT correlation values (*vxy*):

$$\textit{w-statistic} = 1085,\ \textit{p-value} = 0{,}00011$$
$$\textit{z-score}(w_{min}) = -3{,}87293,\ r(w_{min}) = -0{,}40824$$
$$Median_f - Median_w = -0{,}09546$$

Once again, with a p-value of 0,00011, the Wilcoxon signed-rank test attested a significant difference between the wrist and the finger sensor. The median difference indicated a greater resemblance for the wrist sensor derived values compared to the finger sensor based values. Furthermore, an effect size between the 0.3 and 0.5 increment states that the sensor location has large effect on the correlation distribution. Similar results were observed for the other two similarity tests.

6.3.4 Summary and discussion

As shown in Figure 6.3 the wrist based sensor seemed to provide overall higher correlation values for the acquired dataset. In 12 out of 16 significant similarity distribution comparisons it provided higher median values. All the significant distribution tests displayed a medium or large effect based on their computed *r* values. Therefore it can be concluded, that during the course of the conducted user study the sensor located on the wrist of a participant provided more similar signal values than the sensor located on the finger.

Similarity test	Sensor location	x	y	z	vxyz	vxy	vxz	vyz	higher mean count
Pearson correlation	finger	0,37511	0,44474	0,21854	0,65142	0,48921	0,48474	0,65926	2
	wrist	0,57117	0,68588	-0,05393	0,60338	0,56433	0,50911	0,72439	4
FFT correlation	finger	0,47746	0,43406	0,38840	0,73950	0,60397	0,62411	0,69486	1
	wrist	0,64013	0,75537	0,24647	0,71289	0,69942	0,63356	0,66795	3
Velocity correlation	finger	0,84542	0,92906	-0,32365	0,94265	0,57056	0,43449	0,95083	1
	wrist	0,96797	0,95795	-0,23364	0,92256	0,81819	0,81965	0,98353	5

Legend	higher mean	not significant

Figure 6.3: Median values colored by statistical significance. Higher median values are highlighted in green. The tests results with an effect size below r=0.01 were also marked as not significant.

In detail, the finger based sensor only returned higher median correlation values for the z-axis signal and performed less good on the x and y related signals. This result can be aligned with the concept of wrist induced signal disparity. Especially, when it is considered that the wrist can move and fold more easily along x-axis than along the y- and z-axis. It even might be an indicator for a stronger coupling of the finger located sensors. Although, the overall results of the conducted study suggest differently.

Further interesting observations were made when comparing the performance of the selected similarity tests. While returning robust test values on y related signals the FFTP-CWW based similarity test did not provide significantly different correlations on x and z related signals. This lack of performance might be linked to the sample rate. As a frequency based test the FFT relies heavily on a sufficient sample rate to measure fast movements. While the amplitude of the movement along the y-axis is rather distinct the movement in the other two directions is smaller and faster. Admittedly, this assumption is rather speculative but it might be an idea to follow upon.

Besides, the velocity derived similarity test worked very well with most signals. It returned high overall correlation values and large effect sizes. A possible reason for this performance could be the integration step. Since, the applied integration function is an approximation it can be considered an additional preprocessing step that smoothes the signal and filters noise.

A final remark has to be made about the performance of different signals. When looking at the correlation values and the test performance the y, x and vxy signals stood out. This is obviously connected to the earlier stated fact that the up and down motion along the y-axis is more distinct than the movement on the other two axes. Furthermore, this observation is congruent with the findings of the Shakecast project.

7 Conclusion and Future Work

The utilization of a greeting gesture as a trigger to exchange digital information can be a very useful tool. Yet, especially in an scenario where personal information is transferred it is very important to ensure a directed exchange between the concerned parties. The goal of this thesis was to explore an alternate sensor position to improve the performance of directed gesture triggered data exchange. The research was based on the assumption that in the case of a handshake, the tension in the wrist joint has a great impact on the resemblance of the measured acceleration signals. Therefore two sensor locations were compared with several features and similarity measures.

However, the results of the derived comparisons between the wrist sensor and the finger sensor suggested that wrist induced disparity does not have a big influence on the similarity of corresponding acceleration signals. There are some possible reasons for this result. First, based on the observations during the conducted user study it is a possibility that the unnatural situation of a wired arm and a instructed handshake influenced the performance of the participants. Second, as reported during three of the recording sessions the finger mount loosened sometimes. Obviously, a loose mount would diminish the similarity of the acceleration signals. Finally, it was stated several times time that the user touched the sensor of his partner while performing the handshake. Even though all these reasons might only hold true for a part of the recordings, they suggest that there is still room for the possibility that sensor on the finger can perform better than a wrist based sensor.

Accordingly, it would be a good start for future research to move from a wired prototype to an actual ring formed sensor that is less obtrusive and can be used in day to day live. This would also bear the possibility to further explore the use of low range technologies. Most of the deployed hardware was selected to later be installed on a PCB. Therefore, the hardware setup that was developed for this thesis could provide a good starting point. It might also be interesting to examine the three similarity measures and thoroughly test them on their overall performance. Finally, another interesting approach would be to explore the results of an improved version of this setup for a dataset that contains solely handshakes recorded with a low wrist tension. Certainly, gesture based applications still provide plenty of interesting topics that to be investigated in the future.

Bibliography

[1] R. E. Riggio, H. S. Friedman, and M. R. DiMatteo, "Nonverbal greetings: Effects of the situation and personality," *Personality and Social Psychology Bulletin*, vol. 7, no. 4, pp. 682–689, 1981.

[2] J. Åström, "Introductory greeting behaviour: A laboratory investigation of approaching and closing salutation phases," *Perceptual and Motor Skills*, vol. 79, no. 2, pp. 863–897, 1994.

[3] P. M. Hall and D. A. SPENCER HALL, "The handshake as interaction," *Semiotica*, vol. 45, no. 3-4, pp. 249–264, 1983.

[4] J. Huwer, "Understanding handshaking: the result of contextual, interpersonal and social demands," 2003.

[5] B. SCHORSCH, D. Shoemaker, E. Dvortsov, and K. KUDCHADKAR, "Gesture-based information exchange between devices in proximity," 2016. EP Patent App. EP20,130,824,427.

[6] K. Hinckley, "Synchronous gestures for multiple persons and computers," in *Proceedings of the 16th Annual ACM Symposium on User Interface Software and Technology*, UIST '03, (New York, NY, USA), pp. 149–158, ACM, 2003.

[7] M. Kanis, N. Winters, S. Agamanolis, A. Gavin, and C. Cullinan, "Toward wearable social networking with iband," in *CHI '05 Extended Abstracts on Human Factors in Computing Systems*, CHI EA '05, (New York, NY, USA), pp. 1521–1524, ACM, 2005.

[8] T. G. Zimmerman, "Personal area networks: near-field intrabody communication," *IBM systems Journal*, vol. 35, no. 3.4, pp. 609–617, 1996.

[9] A. Augimeri, G. Fortino, M. R. Rege, V. Handziski, and A. Wolisz, "A cooperative approach for handshake detection based on body sensor networks," in *Systems Man and Cybernetics (SMC), 2010 IEEE International Conference on*, pp. 281–288, IEEE, 2010.

[10] T. Weißker, E. Genc, A. Berst, F. D. Schreiber, and F. Echtler, "Shakecast: Using handshake detection for automated, setup-free exchange of contact data," 2017.

[11] R. Want, "Near field communication," *IEEE Pervasive Computing*, vol. 10, no. 3, pp. 4–7, 2011.

[12] Elechouse, "PN532 NFC RFID Module User Guide," 2013.

[13] A. Melnyk, V. P. Borysenko, and P. Henaff, "Analysis of synchrony of a handshake between humans," in *Advanced Intelligent Mechatronics (AIM), 2014 IEEE/ASME International Conference on*, pp. 1753–1758, IEEE, 2014.

[14] Aimee Ferouge, *Handshake Recognition Applied to Wireless Data Exchange in Smartbands*. Master's thesis in embedded systems, Delft University of Technology, Delft, 09.12.2015.

[15] D. Meschede, *Gerthsen physik*. Springer-Verlag, 2015.

[16] G. Tagne, P. Hénaff, and N. Gregori, "Measurement and analysis of physical parameters of the handshake between two persons according to simple social contexts," in *Intelligent Robots and Systems (IROS), 2016 IEEE/RSJ International Conference on*, pp. 674–679, IEEE, 2016.

[17] Z. Wang, E. Giannopoulos, M. Slater, A. Peer, and M. Buss, "Handshake: Realistic human-robot interaction in haptic enhanced virtual reality," *Presence: Teleoperators and Virtual Environments*, vol. 20, no. 4, pp. 371–392, 2011.

[18] J. Benesty, J. Chen, Y. Huang, and I. Cohen, "Pearson correlation coefficient," in *Noise reduction in speech processing*, pp. 1–4, Springer, 2009.

[19] S. J. Orfanidis, *Introduction to signal processing*. Prentice-Hall, Inc., 1995.

[20] B. Sensortec, "BNO055 Intelligent 9-axis absolute orientation sensor," 2014.

[21] K. Karami, "Maximizing ble throughput on ios and android." `https://punchthrough.com/blog/posts/maximizing-ble-throughput-on-ios-and-android`. Accessed: 2017-08-01.

[22] A. Field, *Discovering statistics using IBM SPSS statistics*. Sage, 2013.

[23] T. S. community, "Statistical functions (scipy.stats)." `https://docs.scipy.org/doc/scipy/reference/stats.html`. Accessed: 2017-08-01.

[24] S. S. Shapiro and M. B. Wilk, "An analysis of variance test for normality (complete samples)," *Biometrika*, vol. 52, no. 3/4, pp. 591–611, 1965.

[25] F. Wilcoxon, "Individual comparisons by ranking methods," *Biometrics bulletin*, vol. 1, no. 6, pp. 80–83, 1945.

[26] J. Cohen, "A power primer.," *Psychological bulletin*, vol. 112, no. 1, p. 155, 1992.

A | Appendix

A.1 Similarity test metrics - finger sensor

Applied test	Finger, normal data			n = 90		Finger, control data			n = 8010		Differences: Finger, normal - control				
x	mean	median	minimum	maximum	range	mean	median	minimum	maximum	range	mean	median	minimum	maximum	range
Normalized correlation	0,81281	0,84323	0,46614	0,97132	0,50518	0,772065	0,79271	0,217098	0,971974	0,754876	0,04075	0,05052	0,24904	-0,00066	-0,24970
Pearson correlation	0,35494	0,37511	-0,20179	0,81036	1,01215	0,205274	0,196171	-0,545525	0,833509	1,379034	0,14967	0,17894	0,34374	-0,02315	-0,36689
Peak distance correlation (max)	0,77199	0,78084	0,41216	0,96472	0,55256	0,738115	0,745724	0,261317	1	0,738683	0,03388	0,03512	0,15084	-0,03528	-0,18612
Peak distance correlation (min)	0,72248	0,75949	0,37800	0,99380	0,61580	0,714219	0,726407	0,277852	1	0,722148	0,00826	0,03308	0,10015	-0,00620	-0,10634
FFT correlation	0,414052	0,477456	-0,33952	0,896438	1,23596	0,297034	0,313631	-0,646946	1	1,646946	0,11702	0,16383	0,30743	-0,10356	-0,41099
Velocity correlation	0,67770	0,84542	-0,92062	0,98516	1,90577	0,435769	0,572761	-0,912589	0,994604	1,907193	0,24193	0,27266	-0,00803	-0,00945	-0,00142
Distance correlation	0,98063	0,98964	0,88940	0,99932	0,10992	0,972771	0,980998	0,698178	0,999983	0,301805	0,00786	0,00864	0,19122	-0,00066	-0,19188
y	mean	median	minimum	maximum	range	mean	median	minimum	maximum	range	mean	median	minimum	maximum	range
Normalized correlation	0,40200	0,46131	-0,55365	0,88695	1,44061	0,257587	0,277322	-0,583522	0,872625	1,456147	0,14441	0,18399	0,02987	0,01433	-0,01554
Pearson correlation	0,44474	0,47060	-0,13670	0,85921	0,99591	0,248495	0,248937	-0,438697	0,840955	1,279652	0,19624	0,22166	0,30199	0,01825	-0,28374
Peak distance correlation (max)	0,76530	0,78273	0,45391	0,97404	0,52013	0,754447	0,769944	0,217751	1	0,782249	0,01085	0,01279	0,23616	-0,02596	-0,26212
Peak distance correlation (min)	0,80742	0,82494	0,38982	0,98888	0,59906	0,790825	0,804216	0,27516	1	0,72484	0,01659	0,02072	0,11466	-0,01112	-0,12578
FFT correlation	0,402653	0,43406	-0,623726	0,932081	1,55581	0,188773	0,193882	-0,766831	1	1,766831	0,21388	0,24018	0,14311	-0,06792	-0,21102
Velocity correlation	0,83381	0,92906	-0,22399	0,99169	1,21568	0,630534	0,797856	-0,954481	0,999553	1,954034	0,20328	0,13121	0,73049	-0,00786	-0,73835
Distance correlation	0,98385	0,99249	0,89211	0,99976	0,10765	0,970026	0,980024	0,820834	0,999965	0,179131	0,01382	0,01247	0,07128	-0,00020	-0,07148
z	mean	median	minimum	maximum	range	mean	median	minimum	maximum	range	mean	median	minimum	maximum	range
Normalized correlation	0,55587	0,61638	-0,63343	0,88332	1,51675	0,493772	0,523452	-0,583272	0,908246	1,491518	0,06210	0,09293	-0,05016	-0,02493	0,02523
Pearson correlation	0,21854	0,26286	-0,63349	0,74543	1,37892	0,119658	0,09706	-0,720984	0,808239	1,529223	0,09889	0,16580	0,08750	-0,06281	-0,15031
Peak distance correlation (max)	0,71587	0,71459	0,38775	0,99639	0,60864	0,726116	0,736489	0,238498	1	0,761502	-0,01025	-0,02190	0,14925	-0,00361	-0,15286
Peak distance correlation (min)	0,73998	0,76766	0,44481	0,97188	0,52707	0,731641	0,748516	0,257193	1	0,742807	0,00834	0,01914	0,18762	-0,02812	-0,21574
FFT correlation	0,369201	0,388397	-0,482454	0,888273	1,37073	0,215558	0,224855	-0,781461	1	1,781461	0,15364	0,16354	0,29901	-0,11173	-0,41073
Velocity correlation	-0,21808	-0,32365	-0,97536	0,93571	1,91107	-0,024236	-0,056819	-0,983042	0,99442	1,977462	-0,19385	-0,26683	0,00768	-0,05871	-0,06640
Distance correlation	0,96665	0,97639	0,83377	0,99942	0,16566	0,96533	0,975576	0,699472	0,999993	0,300521	0,00132	0,00081	0,13430	-0,00057	-0,13486
vxyz	mean	median	minimum	maximum	range	mean	median	minimum	maximum	range	mean	median	minimum	maximum	range
Normalized correlation	0,93383	0,94242	0,71463	0,98463	0,27000	0,876603	0,881453	0,680539	0,979488	0,298949	0,05722	0,06097	0,03409	0,00514	-0,02895
Pearson correlation	0,61114	0,65142	-0,11560	0,87340	0,98900	0,305765	0,320428	-0,242835	0,835074	1,077909	0,30538	0,33099	0,12724	0,03832	-0,08891
Peak distance correlation (max)	0,84698	0,85828	0,65745	0,97616	0,31871	0,815745	0,823079	0,523276	1	0,476724	0,03124	0,03520	0,13417	-0,02384	-0,15802
Peak distance correlation (min)	0,81084	0,85221	0,43217	0,99993	0,56776	0,720804	0,721741	0,255935	1	0,744065	0,09003	0,13047	0,17624	-0,00007	-0,17631
FFT correlation	0,688793	0,739504	0,190201	0,964869	0,77467	0,33122	0,344966	-0,448664	1	1,448664	0,35757	0,39454	0,63887	-0,03513	-0,67400
Velocity correlation	0,85031	0,94265	-0,36458	0,99556	1,36014	0,564333	0,704949	-0,861944	0,999052	1,860996	0,28598	0,23771	0,49737	-0,00349	-0,50086
Distance correlation	0,99250	0,99754	0,90467	0,99988	0,09522	0,985176	0,990201	0,832484	0,999993	0,167509	0,00733	0,00734	0,07218	-0,00011	-0,07229
vxy	mean	median	minimum	maximum	range	mean	median	minimum	maximum	range	mean	median	minimum	maximum	range
Normalized correlation	0,90013	0,90827	0,72646	0,96862	0,24216	0,857088	0,863238	0,475006	0,977376	0,50237	0,04304	0,04503	0,25145	-0,00876	-0,26021
Pearson correlation	0,42378	0,48921	-0,14944	0,75778	0,90722	0,205514	0,202886	-0,451292	0,841953	1,293245	0,21827	0,28633	0,30185	-0,08417	-0,38602
Peak distance correlation (max)	0,78686	0,81566	0,31592	0,96641	0,65049	0,774005	0,795103	0,292447	1	0,707553	0,01286	0,02056	0,02347	-0,03359	-0,05707
Peak distance correlation (min)	0,75168	0,77013	0,32645	0,99811	0,67166	0,687105	0,705866	0,228324	1	0,771676	0,06457	0,06426	0,09812	-0,00189	-0,10001
FFT correlation	0,543697	0,603967	-0,074826	0,941784	1,01661	0,285232	0,294669	-0,50999	1	1,50999	0,25847	0,30930	0,43516	-0,05822	-0,49338
Velocity correlation	0,40966	0,57056	-0,84741	0,99473	1,84214	0,201697	0,244721	-0,965696	0,998208	1,963904	0,20796	0,32584	0,11829	-0,00348	-0,12176
Distance correlation	0,97962	0,98551	0,86250	0,99950	0,13700	0,97597	0,982442	0,808649	0,999969	0,19132	0,00365	0,00307	0,05385	-0,00047	-0,05432
vxz	mean	median	minimum	maximum	range	mean	median	minimum	maximum	range	mean	median	minimum	maximum	range
Normalized correlation	0,91737	0,92495	0,68656	0,97844	0,29188	0,874579	0,879965	0,68376	0,980213	0,296453	0,04279	0,04498	0,00280	-0,00178	-0,00458
Pearson correlation	0,46927	0,48474	-0,10246	0,85195	0,95441	0,207963	0,193199	-0,473892	0,835124	1,309016	0,26131	0,29155	0,37143	0,01682	-0,35461
Peak distance correlation (max)	0,76179	0,80339	0,42277	0,98098	0,55820	0,737359	0,760011	0,263624	1	0,736376	0,02443	0,04338	0,15915	-0,01902	-0,17817
Peak distance correlation (min)	0,71891	0,73185	0,30249	0,99789	0,69540	0,659774	0,668367	0,200172	1	0,799828	0,05913	0,06348	0,10232	-0,00211	-0,10443
FFT correlation	0,579055	0,624111	0,051904	0,939484	0,88758	0,332407	0,354432	-0,496686	1	1,496686	0,24665	0,26968	0,54859	-0,06052	-0,60911
Velocity correlation	0,37953	0,43449	-0,72192	0,98785	1,70976	0,129558	0,134738	-0,968916	0,999185	1,968101	0,24997	0,29975	0,24700	-0,01134	-0,25834
Distance correlation	0,97518	0,98411	0,87556	0,99971	0,12415	0,974414	0,981396	0,78408	0,999992	0,215912	0,00077	0,00271	0,09148	-0,00029	-0,09176
vyz	mean	median	minimum	maximum	range	mean	median	minimum	maximum	range	mean	median	minimum	maximum	range
Normalized correlation	0,87185	0,88600	0,49173	0,95430	0,46257	0,779526	0,793887	0,354421	0,957959	0,603538	0,09232	0,09211	0,13731	-0,00366	-0,14097
Pearson correlation	0,61975	0,65926	-0,20594	0,88719	1,09312	0,361045	0,404451	-0,393409	0,89179	1,285199	0,25870	0,25481	0,18747	-0,00460	-0,19208
Peak distance correlation (max)	0,81692	0,82940	0,54024	0,99026	0,45002	0,79632	0,809865	0,405101	1	0,594899	0,02060	0,01953	0,13514	-0,00974	-0,14488
Peak distance correlation (min)	0,80984	0,82709	0,42319	0,99131	0,56811	0,768891	0,772755	0,271791	1	0,728209	0,04095	0,05434	0,15140	-0,00869	-0,16009
FFT correlation	0,67202	0,694855	0,16863	0,947436	0,77881	0,342488	0,356404	-0,500056	1	1,500056	0,32953	0,33845	0,66869	-0,05256	-0,72125
Velocity correlation	0,86867	0,95083	-0,59480	0,99445	1,58925	0,662951	0,843314	-0,924647	0,999018	1,923665	0,20572	0,10751	0,32985	-0,00457	-0,33442
Distance correlation	0,98488	0,99437	0,89280	0,99988	0,10708	0,975766	0,984961	0,782699	0,999993	0,217294	0,00911	0,00941	0,11010	-0,00011	-0,11021

Figure A.1: Metrics for the similarity test distributions ordered by signal and group. The data was recorded with a sensor located on the finger.

A.2 Similarity test metrics - wrist sensor

Applied test	Wrist, normal data			n = 90		Wrist, control data			n = 8010		Differences: Wrist, normal - control				
	x														
	mean	median	minimum	maximum	range	mean	median	minimum	maximum	range	mean	median	minimum	maximum	range
Normalized correlation	0,84885	0,89342	0,29877	0,97728	0,67851	0,790205	0,814937	0,06853	0,98794	0,91941	0,05865	0,07848	0,23024	-0,01066	-0,24090
Pearson correlation	0,53086	0,57117	-0,17543	0,93613	1,11155	0,322975	0,349457	-0,608019	0,941402	1,549421	0,20788	0,22171	0,43259	-0,00527	-0,43787
Peak distance correlation (max)	0,69698	0,71032	0,17370	0,99097	0,81727	0,66033	0,656518	0,168235	1	0,831765	0,03665	0,05380	0,00546	-0,00903	-0,01449
Peak distance correlation (min)	0,83115	0,88558	0,25646	0,99887	0,74242	0,783355	0,813196	0,15757	1	0,84243	0,04780	0,07238	0,09889	-0,00113	-0,10001
FFT correlation	0,579379	0,640129	-0,193681	0,954193	1,14787	0,425821	0,462593	-0,750832	1	1,750832	0,15356	0,17754	0,55715	-0,04581	-0,60296
Velocity correlation	0,90660	0,96797	-0,16581	0,99735	1,16316	0,621792	0,797498	-0,975782	0,999694	1,975476	0,28481	0,17047	0,80998	-0,00234	-0,81232
Distance correlation	0,99265	0,99680	0,89526	0,99991	0,10465	0,978719	0,984546	0,82277	0,999972	0,177202	0,01393	0,01226	0,07249	-0,00006	-0,07255
	y														
	mean	median	minimum	maximum	range	mean	median	minimum	maximum	range	mean	median	minimum	maximum	range
Normalized correlation	0,77578	0,82535	0,20186	0,95452	0,75266	0,619997	0,639431	-0,182747	0,965772	1,148519	0,15578	0,18592	0,38461	-0,01125	-0,39586
Pearson correlation	0,58868	0,68588	-0,01792	0,87806	0,89598	0,297146	0,297556	-0,509878	0,925667	1,435545	0,29153	0,38833	0,49195	-0,04761	-0,53956
Peak distance correlation (max)	0,79445	0,81669	0,39458	0,97805	0,58347	0,749894	0,762974	0,261057	1	0,738943	0,04455	0,05372	0,13353	-0,02195	-0,15547
Peak distance correlation (min)	0,84930	0,88087	0,40816	0,99157	0,58341	0,813365	0,827428	0,248656	1	0,751344	0,03593	0,05344	0,15950	-0,00843	-0,16794
FFT correlation	0,648348	0,755367	-0,329262	0,976254	1,30552	0,379893	0,430115	-0,792087	1	1,792087	0,26846	0,32525	0,46283	-0,02375	-0,48657
Velocity correlation	0,89483	0,95795	-0,13648	0,99566	1,13214	0,663189	0,823101	-0,969526	0,999286	1,968812	0,23164	0,13485	0,83305	-0,00362	-0,83667
Distance correlation	0,98731	0,99533	0,87579	0,99986	0,12408	0,969876	0,979773	0,780593	0,99994	0,219347	0,01743	0,01556	0,09520	-0,00008	-0,09527
	z														
	mean	median	minimum	maximum	range	mean	median	minimum	maximum	range	mean	median	minimum	maximum	range
Normalized correlation	-0,05305	-0,03012	-0,79559	0,67333	1,46892	0,061195	0,071914	-0,872071	0,834102	1,706173	-0,11425	-0,10203	0,07648	-0,16077	-0,23725
Pearson correlation	-0,07565	-0,05393	-0,66652	0,66107	1,32759	0,006501	0,006248	-0,729764	0,833034	1,562798	-0,08215	-0,06018	0,06324	-0,17197	-0,23521
Peak distance correlation (max)	0,69450	0,68709	0,29289	0,98196	0,68907	0,708179	0,729316	0,209183	1	0,790817	-0,01368	-0,04222	0,08371	-0,01804	-0,10175
Peak distance correlation (min)	0,72495	0,73064	0,35892	0,96602	0,60711	0,732958	0,749721	0,18369	1	0,81631	-0,00801	-0,01908	0,17523	-0,03398	-0,20920
FFT correlation	0,250465	0,246466	-0,539147	0,905337	1,44448	0,132111	0,134129	-0,781945	1	1,781945	0,11835	0,11234	0,24280	-0,09466	-0,33746
Velocity correlation	-0,11021	-0,23364	-0,95545	0,93509	1,89055	0,014347	0,014758	-0,990065	0,998578	1,988643	-0,12456	-0,24840	0,03461	-0,06348	-0,09810
Distance correlation	0,96619	0,97863	0,84673	0,99882	0,15209	0,966544	0,975106	0,760179	0,999968	0,239789	-0,00035	0,00353	0,08655	-0,00114	-0,08770
	vxyz														
	mean	median	minimum	maximum	range	mean	median	minimum	maximum	range	mean	median	minimum	maximum	range
Normalized correlation	0,93964	0,95268	0,72190	0,98883	0,26693	0,894015	0,899173	0,704996	0,988992	0,283996	0,04562	0,05350	0,01690	-0,00017	-0,01707
Pearson correlation	0,55777	0,60338	-0,11454	0,88357	0,99812	0,253115	0,25425	-0,332306	0,895919	1,228225	0,30466	0,34913	0,21776	-0,01235	-0,23011
Peak distance correlation (max)	0,84161	0,84745	0,62976	0,99235	0,36259	0,817636	0,827163	0,354162	1	0,645838	0,02398	0,02029	0,27559	-0,00765	-0,28325
Peak distance correlation (min)	0,78736	0,79676	0,21697	0,99878	0,78180	0,690746	0,68783	0,211657	1	0,788343	0,09661	0,10893	0,00532	-0,00122	-0,00654
FFT correlation	0,668115	0,712894	-0,001545	0,96977	0,97132	0,320624	0,33188	-0,546321	1	1,546321	0,34749	0,38101	0,54478	-0,03023	-0,57501
Velocity correlation	0,80686	0,92256	-0,32340	0,99505	1,31844	0,425099	0,493389	-0,812164	0,998658	1,810822	0,38176	0,42917	0,48877	-0,00361	-0,49238
Distance correlation	0,99476	0,99761	0,96944	0,99988	0,03044	0,986602	0,991132	0,855641	0,999993	0,144352	0,00816	0,00648	0,11380	-0,00011	-0,11391
	vxy														
	mean	median	minimum	maximum	range	mean	median	minimum	maximum	range	mean	median	minimum	maximum	range
Normalized correlation	0,93337	0,94108	0,72668	0,98397	0,25729	0,890342	0,895621	0,708532	0,985044	0,276512	0,04303	0,04546	0,01815	-0,00107	-0,01922
Pearson correlation	0,51695	0,56433	-0,10316	0,82998	0,93314	0,228363	0,222141	-0,331075	0,885479	1,216554	0,28858	0,34219	0,22791	-0,05550	-0,28341
Peak distance correlation (max)	0,81209	0,83346	0,45633	0,98064	0,52431	0,791401	0,810476	0,342523	1	0,657477	0,02069	0,02298	0,11381	-0,01936	-0,13317
Peak distance correlation (min)	0,75996	0,79209	0,21697	0,99721	0,78023	0,677155	0,67655	0,171589	1	0,828411	0,08280	0,11554	0,04539	-0,00279	-0,04818
FFT correlation	0,631354	0,699424	-0,04935	0,94427	0,99362	0,302335	0,315888	-0,569324	1	1,569324	0,32902	0,38354	0,51997	-0,05573	-0,57570
Velocity correlation	0,66431	0,81819	-0,48144	0,99248	1,47392	0,290116	0,330864	-0,907791	0,998338	1,906129	0,37420	0,48732	0,42635	-0,00586	-0,43221
Distance correlation	0,98943	0,99536	0,89771	0,99988	0,10217	0,981241	0,98878	0,78799	0,999992	0,212002	0,00818	0,00658	0,10972	-0,00011	-0,10983
	vxz														
	mean	median	minimum	maximum	range	mean	median	minimum	maximum	range	mean	median	minimum	maximum	range
Normalized correlation	0,92700	0,93907	0,68825	0,98373	0,29548	0,881825	0,885496	0,610051	0,990515	0,380464	0,04517	0,05358	0,07820	-0,00679	-0,08499
Pearson correlation	0,50183	0,50911	-0,33179	0,93309	1,26487	0,200234	0,184259	-0,515486	0,920662	1,436148	0,30160	0,32485	0,18370	0,01243	-0,17127
Peak distance correlation (max)	0,78741	0,84302	0,35414	0,99168	0,63754	0,719479	0,744732	0,140979	1	0,859021	0,06794	0,09829	0,21316	-0,00832	-0,22148
Peak distance correlation (min)	0,73607	0,75352	0,17619	0,99653	0,82034	0,698095	0,712833	0,107957	1	0,892043	0,03798	0,04068	0,06824	-0,00347	-0,07170
FFT correlation	0,617127	0,633557	-0,054283	0,932296	0,98658	0,428329	0,447839	-0,521871	1	1,521871	0,18880	0,18572	0,46759	-0,06770	-0,53529
Velocity correlation	0,66939	0,81965	-0,80185	0,99796	1,79981	0,358701	0,445919	-0,972431	0,999608	1,972039	0,31068	0,37373	0,17058	-0,00165	-0,17223
Distance correlation	0,97787	0,98904	0,85018	0,99988	0,14970	0,970301	0,978314	0,755198	0,999979	0,244781	0,00757	0,01073	0,09498	-0,00010	-0,09508
	vyz														
	mean	median	minimum	maximum	range	mean	median	minimum	maximum	range	mean	median	minimum	maximum	range
Normalized correlation	0,87698	0,89262	0,50240	0,96219	0,45979	0,785968	0,804069	0,284204	0,977098	0,692894	0,09101	0,08855	0,21819	-0,01491	-0,23310
Pearson correlation	0,67214	0,72439	-0,06500	0,89429	0,95929	0,414866	0,467277	-0,502689	0,938565	1,441254	0,25727	0,25711	0,43769	-0,04427	-0,48196
Peak distance correlation (max)	0,80280	0,80702	0,50767	0,98089	0,47321	0,749151	0,762555	0,312407	1	0,687593	0,05365	0,04447	0,19527	-0,01911	-0,21438
Peak distance correlation (min)	0,83579	0,85347	0,43646	0,99406	0,55760	0,799439	0,808592	0,336327	1	0,663673	0,03635	0,04487	0,10013	-0,00594	-0,10607
FFT correlation	0,626272	0,667948	-0,035883	0,936686	0,97257	0,307232	0,309677	-0,513562	1	1,513562	0,31904	0,35827	0,47768	-0,06331	-0,54099
Velocity correlation	0,92797	0,98353	-0,16660	0,99674	1,16334	0,689889	0,862011	-0,966711	0,999639	1,96635	0,23808	0,12152	0,80011	-0,00290	-0,80301
Distance correlation	0,99246	0,99728	0,86597	0,99993	0,13396	0,972794	0,985036	0,696198	0,999959	0,303761	0,01966	0,01225	0,16977	-0,00003	-0,16980

Figure A.2: Metrics for the similarity test distributions ordered by signal and group. The data was recorded with a sensor located on the wrist.

A.3 Results of the Shapiro-Wilk test

Finger	x		y		z		vxyz		vxy		vxz		vyz	
similarity test	statistic	p-value	statistic	p-value	statistic	p-value	statistic	p-value	statistic	p-value	statistic	p-value	statistic	p-value
Normalized correlation	0,886667	0,000001	0,933982	0,000195	0,862225	0	0,700404	0	0,867924	0	0,792345	0	0,735969	0
Pearson correlation	0,953017	0,002582	0,970075	0,035792	0,95734	0,004887	0,857943	0	0,948649	0,001383	0,968037	0,025764	0,793302	0
Pdc maxima	0,952675	0,002457	0,964543	0,014783	0,989627	0,703706	0,955378	0,003649	0,908192	0,00001	0,937678	0,000313	0,975932	0,093186
Pdc minima	0,953123	0,002622	0,930838	0,000131	0,955801	0,003885	0,900206	0,000004	0,960604	0,008016	0,962382	0,010545	0,929432	0,00011
FFT correlation	0,972995	0,057591	0,946499	0,001024	0,911859	0,000014	0,914114	0,000018	0,942999	0,000634	0,954428	0,003173	0,929937	0,000118
Velocity correlation	0,716062	0	0,616388	0	0,900433	0,000004	0,575102	0	0,879071	0,000001	0,91079	0,000013	0,457514	0
Distnace correlation	0,780837	0	0,738654	0	0,784302	0	0,508865	0	0,776573	0	0,808588	0	0,670808	0

p = 0 if p < 0,00001

Wrist	x		y		z		vxyz		vxy		vxz		vyz	
similarity test	statistic	p-value	statistic	p-value	statistic	p-value	statistic	p-value	statistic	p-value	statistic	p-value	statistic	p-value
Normalized correlation	0,773759	0	0,829055	0	0,979712	0,172442	0,761211	0	0,824874	0	0,817389	0	0,709953	0
Pearson correlation	0,955919	0,003954	0,851729	0	0,977297	0,116514	0,89555	0,000003	0,906673	0,000008	0,967887	0,02515	0,744989	0
Pdc maxima	0,963633	0,012816	0,901363	0,000005	0,98853	0,622937	0,974844	0,077974	0,877439	0	0,900938	0,000004	0,952899	0,002538
Pdc minima	0,771021	0	0,898167	0,000003	0,978983	0,153297	0,941243	0,000501	0,942587	0,0006	0,949261	0,001507	0,9107	0,000013
FFT correlation	0,986342	0,471413	0,829419	0	0,98219	0,255507	0,941532	0,000521	0,925494	0,000068	0,980947	0,210105	0,922968	0,000051
Velocity correlation	0,397156	0	0,469037	0	0,93375	0,000189	0,689768	0	0,782341	0	0,780726	0	0,330617	0
Distnace correlation	0,395074	0	0,557634	0	0,816406	0	0,712217	0	0,604995	0	0,715724	0	0,390811	0

p = 0 if p < 0,00001

Figure A.3: Results for the Shapiro-Wilk test ordered by signal and similarity test.

A.4 Results of the Wilcoxon signed-rank test

		x	y	z	vxyz	vxy	vxz	vyz
Pearson correlation	statistic	848	594	775	1247	875	1735	1014
	p-value	0,00001	0,00001	0,00001	0,00128	0,00001	0,20861	0,00003
	z-score	-4,82657	-5,84862	-5,12031	-3,22107	-4,71793	-1,25744	-4,15862
	r	-0,50877	-0,61650	-0,53973	-0,33953	-0,49731	-0,13255	-0,43836
	mean(f)-mean(w)	-0,19605	-0,24115	0,27248	0,04803	-0,07511	-0,02437	-0,06513
FFT correlation	statistic	1653	558	1180	1812	1085	1206	1853
	p-value	0,11243	0,00001	0,00048	0,34334	0,00011	0,00071	0,43386
	z-score	-1,58740	-5,99348	-3,49066	-0,94761	-3,87293	-3,38605	-0,78263
	r	-0,16733	-0,63177	-0,36795	-0,09989	-0,40824	-0,35692	-0,08250
	mean(f)-mean(w)	-0,16267	-0,32131	0,14193	0,02661	-0,09546	-0,00945	0,02691
Velocity correlation	statistic	107	1086	1709	1109	840	981	476
	p-value	0,00001	0,00011	0,17319	0,00016	0,00001	0,00002	0,00001
	z-score	-7,80822	-3,86890	-1,36206	-3,77636	-4,85876	-4,29141	-6,32343
	r	-0,82306	-0,40782	-0,14357	-0,39806	-0,51216	-0,45235	-0,66655
	mean(f)-mean(w)	-0,12255	-0,02888	-0,09001	0,02009	-0,24762	-0,38516	-0,03270

Figure A.4: Results for the Wilcoxon signed-rank test ordered by signal and similarity test.